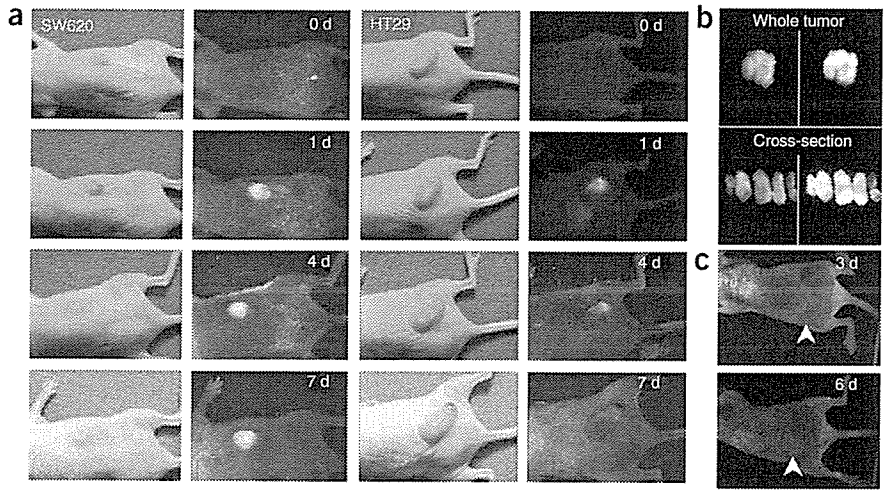

Figure 3 Selective visualization of subcutaneous tumors *in vivo*. (**a**) Time course of external images of subcutaneous SW620 and HT29 tumors after intratumoral injection of OBP-401. When tumors grew to ~6–7 mm in diameter after subcutaneous inoculation of SW620 and HT29 tumor cells (5×10^6 cells per mouse), OBP-401 viruses at the concentration of 1×10^7 PFU were directly injected into established tumors. The GFP fluorescence intensity was monitored for 7 d under the CCD noninvasive imaging system. Left panels, macroscopic appearance of subcutaneous tumors; right panels, fluorescence detection. (**b**) SW620 tumors were excised 14 d after OBP-401 injection and then assessed for GFP fluorescence as a whole tumor or in cross-sections. Left panels, macroscopic appearance of subcutaneous tumors; right panels, fluorescence detection. (**c**) Photographs of non-tumor-bearing *nu/nu* mice injected with OBP-401. Mice were subcutaneously injected with 1×10^7 PFU of OBP-401 and documented as photographs for GFP expression 3 d and 6 d after injection. Arrowheads, injected area.

Orthotopic mouse model of human rectal cancer with metastasis

The development of the orthotopic implantation technique for human rectal cancer has been described[20]. Our preliminary experiments revealed that, when 5×10^6 HT29 human colorectal cancer cells suspended in Matrigel are inoculated into the rectum submucosa of athymic *nu/nu* mice, rectal tumors appeared within 7 d after tumor injection (**Fig. 4a,b**). Histopathological examination of the excised primary tumor showed a submucosal tumor formation composed of implanted HT29 cells with a solid architecture and invasion into the muscularis propria and submucosa (**Fig. 4c**). Examination under high magnification showed tumor cell–filled lymphatic vessels in the muscularis propria layer (**Fig. 4c**). As expected, we detected the green fluorescence expression from 24 h after intratumoral administration of OBP-401 in the primary rectal tumors, with maximum signal occurring 2–4 d after injection, whereas tumors not injected with OBP-401 were completely GFP negative (**Fig. 4d**).

Selective visualization of lymph node metastasis

In our preliminary experiments, we confirmed that most mice with rectal tumors subsequently developed lymph node metastasis around the abdominal aorta from the lower margin of the renal vein to the aortic bifurcation, which were microscopically detectable ~4 weeks after tumor inoculation. Five days after injection of 1×10^8 PFU of OBP-401 into the implanted rectal tumors, we explored the abdominal cavity at laparotomy. Analyses of two representative mice are shown in **Figure 4**. Three lymph nodes (LN1, LN2 and LN3) were macroscopically identified adjacent to the aorta (**Fig. 4e,f**); the optical CCD imaging of the abdominal cavity, however, demonstrated that only one lymph node (LN3) could be detected as light-emitting spots with GFP fluorescence (**Fig. 4f**). In the other mouse, three of four lymph nodes could be imaged as GFP signals (**Fig. 4h**). We detected no GFP fluorescence in abdominal lymph nodes after injection of 1×10^7 PFU of OBP-401 into the rectal tumors (data not shown). Histopathological analysis confirmed the presence of metastatic adenocarcinoma cells in the lymph nodes with fluorescence emission, whereas GFP-negative lymph nodes contained no tumor cells (**Fig. 4g,i**). In addition, immunohistochemical analysis for GFP protein demonstrated that the reddish brown GFP-immunoreactive cells corresponded to the microscopic metastatic nodules in the lymph nodes but were not detected in the nonmetastatic lymphocyte area (**Supplementary Fig. 3** online).

We verified the GFP-based fluorescence detection with OBP-401 and histological correlation of lymph node metastasis in a series of *in vivo* experiments. Representative examples of the data are summarized in **Table 1**. Among the 7 tumor-bearing mice, 6 mice (85.7%) developed histologically confirmed lymph node metastasis. Of 28 lymph nodes excised from 7 mice, histopathological analysis demonstrated that 13 nodes (46.4%) contained micrometastatic nodules. The optical CCD imaging detected 12 lymph nodes labeled in spots with GFP fluorescence in 13 metastatic nodes (sensitivity of 92.3%). Among 15 metastasis-free lymph nodes, 2 nodes were GFP positive (specificity of 86.7%). Our results indicate that intratumoral injection of OBP-401 causes viral spread into the regional lymphatic area and selective replication in cancer cells in metastatic lymph nodes, which in turn could be imaged with GFP fluorescence. Moreover, the finding that OBP-401 did not express GFP fluorescence in a mouse para-aortic lymphadenitis model induced by inoculating complete Freund adjuvant into the rectum submucosa of

Table 1 GFP fluorescence and histopathology status in para-aortic lymph nodes of HT29 tumor-bearing mice

		GFP fluorescence[b]		
Mouse no.	Metastasis[a]	Positive	Negative	Total (%)[c]
1	Positive	1	0	1 (33.3)
	Negative	0	2	2 (66.6)
2	Positive	3	0	3 (75.0)
	Negative	0	1	1 (25.0)
3	Positive	1	0	1 (33.3)
	Negative	0	2	2 (66.6)
4	Positive	0	0	0 (0)
	Negative	0	4	4 (100)
5	Positive	1	1	2 (66.6)
	Negative	0	1	1 (33.3)
6	Positive	3	0	3 (60.0)
	Negative	1	1	2 (40.0)
7	Positive	3	0	3 (50.0)
	Negative	1	2	3 (50.0)

[a]Metastatic foci were detected histologically by hematoxylin and eosin staining. [b]Nodes with light-emitting spots and GFP fluorescence were evaluated as positive. [c]The percentage of nodes with or without histologically confirmed metastasis in each mouse.

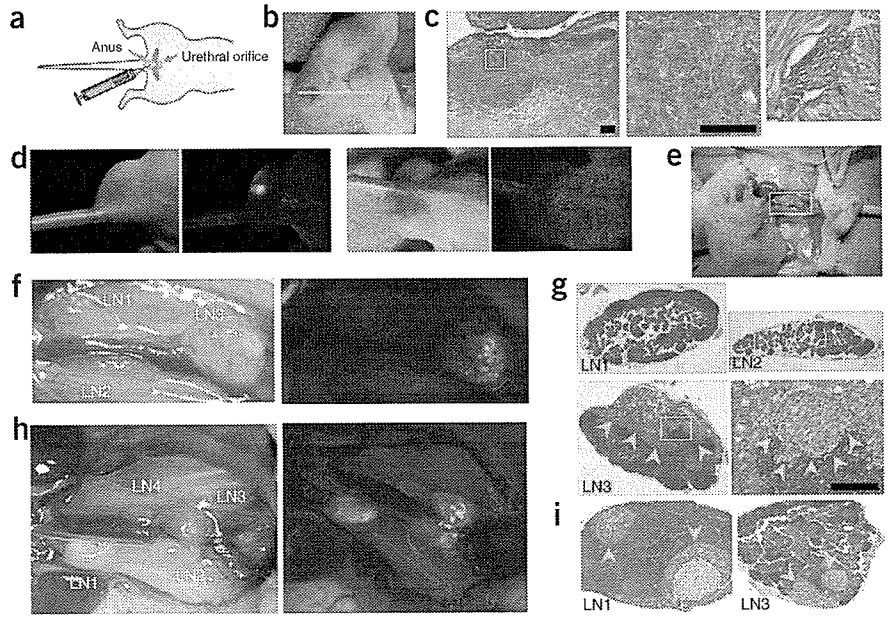

Figure 4 Orthotopic xenografts of human colorectal cancer cells and selective visualization of lymph node metastasis in two representative mice (no. 1 and no. 2). (**a**) Method used to produce HT29 human rectal tumors in BALB/c *nu/nu* mice. The rectums of mice were inoculated with 5×10^6 HT29 cells. (**b**) Macroscopic appearance of HT29 rectal tumor 4 weeks after tumor inoculation. Mice were killed and subjected to autopsy. Green line, the direction of tumor cross-sections. (**c**) Histologic sections stained with H&E showing local growth of HT29 tumor in the submucosal layer of the rectum. Scale bar, 100 μm. Left, magnification: ×40; middle (detail of the boxed region of left panel), magnification: ×400; right, lymphatic vessel invasion of HT29 tumor cells (arrowhead), magnification: ×400. (**d**) External images of orthotopic HT29 tumor-bearing *nu/nu* mice injected with OBP-401. OBP-401 at the concentration of 1×10^8 PFU were directly injected into implanted HT29 tumor (left). The GFP fluorescence could be detected as early as 24 h after OBP-401 injection under CCD imaging. Macroscopic and fluorescent images of HT29 tumor without OBP-401 injection (right). (**e**) Gross appearance of the abdominal cavity (mouse no. 1). At 5 d after intratumoral injection of OBP-401 at the concentration of 1×10^8 PFU, HT29 tumor-bearing *nu/nu* mice were assessed for lymph node metastasis at laparotomy. The white box outlines a region of **f**. (**f**) Three para-aortic lymph nodes were identified in mouse no. 1 (LN1, LN2 and LN3) (left). Internal imaging with the optical CCD camera visualized one of three nodes with GFP fluorescence (LN3) (right). (**g**) H&E staining of lymph node sections. Lymph nodes without metastatic tumors (LN1 and LN2). Lymph node containing metastatic tumors (arrowheads) (LN3) (Left, magnification: ×200; right, magnification: ×400). Scale bar, 100 μm. (**h**) Four para-aortic lymph nodes were identified in mouse no. 2 (LN1, LN2, LN3 and LN4) (left). Three of four nodes were positive for light-emitting spots with GFP fluorescence (LN1, LN2 and LN3) (right). (**i**) Histopathological detection of metastatic foci in nodes (LN1 and LN3) (arrowheads).

immunocompetent BALB/c mice suggests that this strategy could distinguish cancer metastasis from inflammatory lymphadenopathy (**Supplementary Fig. 4** online).

DISCUSSION

Lymph node status provides important information for both the diagnosis and treatment of human cancer[21,22]. Lymphatic invasion is one of the major routes for cancer cell dissemination, and adequate resection of locoregional lymph nodes is required for curative treatment in patients with advanced malignancies. The risk of having lymph node metastasis can be partially predicted by clinical data such as tumor stage, serum tumor marker concentration and medical images; there are, however, no noninvasive approaches to accurately predict the presence of lymph node metastasis, in particular, microscopic metastasis.

The specific aim of the present study was to determine the suitability of telomerase-specific amplification of the *GFP* gene for real-time imaging tumor tissues and, if so, detect nodal metastasis *in vivo* before the traditional, cumbersome procedures of histopathological examination. GFP-based fluorescence imaging can allow real-time detection of target cells without time-consuming steps such as fixation and tissue processing[13–15]. Indeed, Yang *et al.* have shown that GFP-expressing tumors growing and metastasizing in intact animals could be viewed externally with a whole-body optical imaging system[13]. Moreover, the *GFP* gene could be delivered to metastatic tumor cells *in vivo* by viral vectors[14].

To distinguish normal from neoplastic tumor tissues, selective labeling of tumor cells is required. OBP-401 produced a viral yield of 6–7 logs in human cancer cells within 3 d of infection, which was 3–4 logs higher than that in normal cells, suggesting the reliable tumor selectivity of OBP-401. Although the reason why OBP-401 replicated slightly in NHLFs despite the lack of *hTERT* mRNA expression is unclear, the fact that NHLFs could be maintained in the culture up to passages 10–20 indicates that NHLFs might have a weak telomerase activity that is undetectable by standard PCR assay. However, the attenuated replication property of OBP-401 in normal cells seems not to interfere with the visualization of tumor cells *in vivo*. In fact, we detected no GFP expression in adjacent normal tissues in subcutaneous human cancer xenografts after intratumoral injection of OBP-401, although the cross-sections of the tumor were entirely imaged with GFP fluorescence. Thus, OBP-401 provides possible probing of tumor cells *in vivo*.

Experiments using a three-CCD optical imaging system demonstrated that metastatic lymph nodes could be detected at laparotomy in mice 5 d after OBP-401 injection into implanted primary human rectal tumors. Notably, metastatic lymph nodes were imaged in spots with GFP fluorescence, which coincided with histologically confirmed micrometastasis. This experiment mimics the clinical scenario in which patients with gastrointestinal malignancies with lymph node metastasis undergo surgery, and the data suggest that the surgeon can identify metastatic lymph nodes by illuminating the abdominal cavity with a xenon lamp. The sensitivity and specificity of this imaging strategy are 92.3% and 86.7%, respectively; these results are sufficiently reliable to support the concept of this approach. In our phase I trial of a replication-deficient adenovirus vector expressing the wild-type *p53* gene (AdCMV-*p53*, ADVEXIN), DNA-PCR analysis targeting the viral genome indicated that the virus was present in tumor tissue as well as proximal lymph nodes, suggesting regional spread of the vector via the lymphatic vessels[23]. Therefore, OBP-401 is likely to be accessible to the regional lymph nodes via intratumoral administration in humans.

Currently, analysis of lymph nodes with H&E staining and microscopic examination usually involves review of only one or two tissue sections, and small foci of tumor cells can be missed. For intraoperative frozen-section analysis of SLNs, this underestimation is even more pronounced as a result of poor tissue architecture. In the treatment of breast cancer and melanoma, in which SLN biopsy is commonly used, the sensitivity of intraoperative frozen-section analysis ranges from 38% to 74% (refs. 6–9). In our experiments, additional serial sectioning was needed in 4 of 12 (33.3%) lymph nodes with GFP fluorescence to detect micrometastasis. This finding suggests that this GFP-based approach has higher sensitivity for detecting occult lymph node metastasis as compared with standard histopathological examination. Thus, the two GFP-positive nodes, in which tumor cells were not detected histologically, could have contained microscopic metastasis that would have been identified by further sectioning. Other possible explanations of false-positive detection include either that GFP protein itself was produced in the primary tumor spread into regional lymph nodes or that high doses of OBP-401 entered nodes and incidentally replicated in normal lymphocytes in that they have low telomerase activity[24].

Although the molecular imaging strategy using OBP-401 is considered promising, some limitations of the system exist, the main one being the relatively short wavelength of excitation light of GFP. In contrast to luciferase, which is also commonly used for molecular imaging[25], if objects are located in the deep layer or covered with thick adjacent tissues, the excitation light for GFP may not be able to reach them. For example, when tumor foci were exposed to the surface of nodes opposite the illuminated field, GFP fluorescence could not be detected, thereby leading to false-negative detection. The extension of exposure time to the illumination allows increasing the fluorescence intensity; the excitation light, however, cannot penetrate deeper. To raise the imaging sensitivity, one possible approach is to make the specimen thinner, for example, by pressing the excised lymph nodes flat; the architecture of the nodes, however, may be destroyed. Alternatively, it might be useful to develop a hand-held probe, in which the outlet of the excitation beam light and the sensor of GFP fluorescence are combined. During surgery, metastatic lymph nodes could be positively identified with GFP fluorescence guided by this probe like a gamma probe for SLN biopsy. At least, a hand-held flashlight to excite GFP fluorescence has been reported[26].

Administration of OBP-401 can provide an additional advantage in cancer therapy. OBP-401, similar to OBP-301, is an oncolytic virus and selectively kills human tumor cells by viral replication; the process of cell death by OBP-401, however, is relatively slow in comparison with apoptosis-inducing chemotherapeutic drugs, because the virus needs time for replication. Therefore, tumor cells infected with OBP-401 express GFP fluorescence and then lose viability, allowing the timing of detection. We could speculate that OBP-401 would spread into the regional lymph nodes after intratumoral injection, express GFP signals in tumor cells by virus replication and finally kill tumor cells even if the surgeon failed to remove all nodes containing micrometastasis. Thus, the oncolytic activity of OBP-401 may function as a backup safety antitumor program.

In conclusion, we have demonstrated that the GFP-expressing telomerase-specific replication-selective adenovirus OBP-401 can be delivered into human tumor cells in regional lymph nodes and replicate with selective GFP fluorescence after injection into the primary tumor in an orthotopic rectal tumor model. The feasibility of original OBP-301 (Telomelysin) for human cancer therapy will be confirmed in clinical trials in the near future. Because the safety profiles of these two viruses are considered homologous, this molecular imaging strategy using OBP-401 has a potential of being widely available in humans as a navigation system in the surgical treatment of malignancy.

METHODS

Cell culture. The human non-small-cell lung cancer cell lines H1299 and H460, the human gastric cancer cell lines MKN28 and MKN45, the human colorectal cancer cell lines SW620 and HT29, the human esophageal cancer cell lines TE8 and T.Tn, the human prostate cancer cell lines LNCaP and PC-3, the human tongue squamous carcinoma cell lines HSC-3, HSC-4, SCC-4 and SCC-9, the human cervical adenocarcinoma cell line HeLa, the human hepatocellular carcinoma cell line HepG2, the human pancreatic cancer cell line Panc-1, the human mammary gland adenocarcinoma cell line MCF-7, the human osteosarcoma cell line U-2OS (ATCC), the NHLF cell line, the normal human renal epithelial cell line HRE, the human umbilical vascular endothelial cell line HUVEC (TaKaRa Biomedicals) and the normal human lung diploid fibroblast cell line WI38 (HSRRB) were cultured according to the vendor's specifications.

OBP-401. OBP-401 is a telomerase-specific replication-competent adenovirus variant in which the hTERT promoter element drives the expression of *E1A* and *E1B* genes linked with an internal ribosome entry site, with the *GFP* gene inserted under the CMV promoter into the E3 region for monitoring viral replication[27,28]. The virus was purified by ultracentrifugation in cesium chloride step gradients, their titers were determined by a plaque-forming assay using 293 cells and they were stored at –80 °C.

Quantitative real-time PCR analysis. Total RNA from the cultured cells was obtained using the RNeasy Mini Kit (QIAGEN). The *hTERT* mRNA copy number was determined by real-time quantitative RT-PCR using a LightCycler instrument and a LightCycler DNA TeloTAGGG Kit (Roche Molecular Biochemicals). DNA was extracted with the QIAamp DNA Mini Kit (QIAGEN), and quantitative real-time PCR assay for the *E1A* gene was also performed. The sequences of specific primers used for *E1A* were, sense: 5′-CCTGTGTCTAGAGAATGCAA-3′; antisense: 5′-ACAGCTCAAGTCCAAAG GTT-3′. PCR amplification began with a 600-s denaturation step at 95 °C and then 40 cycles of denaturation at 95 °C for 10 s, annealing at 58 °C for 15 s and extension at 72 °C for 8 s. Data analysis was performed using LightCycler Software (Roche Molecular Biochemicals). The ratios normalized by dividing the value of untreated cells were presented for each sample.

Fluorescence microscopy. Human cancer cell lines (H1299, SW620 and HT29) and normal cells (NHLFs) were infected with either 1 or 10 MOI of OBP-401 for 2 h *in vitro*. Expression of the *GFP* gene was assessed and photographed (magnification: ×200) using an Eclipse TS-100 fluorescent microscope (Nikon).

Electron microscopy. Human prostate cancer cell line LNCaP was infected with 10 MOI of OBP-401. Thin sections were cut on coated copper grids and stained with uranyl acetate. The samples were examined and photographed with a Hitachi H-7100 transmission electron microscope.

Immunohistochemistry. Immunohistochemical staining was performed using a Histofine SAB PO kit (Nichirei) according to the manufacturer's instructions. Paired tissues of primary tumors and lymph node metastases were obtained from gastric cancer patients who underwent surgery at Okayama University Hospital. Informed consent was obtained from each individual as approved by the Ethics Review Committee for Clinical Investigation of our institution. Formalin-fixed, paraffin-embedded tissue sections were mounted on silanized slides and deparaffinized. After blocking of nonspecific reactivity with rabbit or goat serum for 10 min at 25 °C, sections were incubated overnight at 4 °C with the monoclonal antibody to hTERT (Kyowa Medex). After rinsing, the slides were incubated with biotinylated rabbit antibody to mouse, and then with avidin-biotin-peroxidase complex. Peroxidase activity was determined using DAB-H_2O_2 solution (Histofine DAB substrate kit; Nichirei). The slides were counterstained with methyl green and Mayer's hematoxylin.

Animal experiments. The experimental protocol was approved by the Ethics Review Committee for Animal Experimentation of our institution. We

produced SW620 and HT29 xenografts on the back in 5-week-old female BALB/c *nu/nu* mice by subcutaneous injection of 5×10^6 SW620 or HT29 cells in 100 μl of HBSS using a 27-gauge needle. When tumors grew to ~6–7 mm in diameter, both tumors were intratumorally injected with OBP-401 (1×10^7 PFU/100 μl). Mice were anesthetized by intraperitoneal injection of pentobarbital (50 mg/kg) and examined for GFP expression. Six mice were used for each tumor cell line. To generate an orthotopic rectal cancer model, female BALB/c *nu/nu* mice were anesthetized and then placed in a supine position. The anorectal wall was cut at a length of 7 mm to prevent colonic obstruction resulting from rectal tumor progression. We injected cell suspension of HT29 cells at a density of 5×10^6 cells in 100 μl of Matrigel basement membrane matrix (Becton Dickinson Labware) slowly into the submucosal layer of the rectum through a 27-gauge needle (**Fig. 4a**). Four weeks later we injected 1×10^8 PFU/100 μl of OBP-401 directly into the rectal tumors. Mice were killed, and their abdominal spaces were examined at laparotomy 5 d after virus injection.

Cooled CCD imaging. *In vivo* GFP fluorescence imaging was acquired by illuminating the animal with a xenon 150-W lamp. The re-emitted fluorescence was collected through a long-pass filter on a Hamamatsu C5810 3-chip color CCD camera (Hamamatsu Photonics Systems). High-resolution images were acquired using an EPSON PC. Images were processed for contrast and brightness with the use of Adobe Photoshop 4.0.1J software (Adobe).

Note: Supplementary information is available on the Nature Medicine website.

ACKNOWLEDGMENTS

This work was supported in part by grants from the Ministry of Education, Culture, Sports, Science, and Technology of Japan (T.F. and S.K.); and by grants from the Ministry of Health, Labour, and Welfare of Japan (T.F.). We thank K. Nagai and H. Kawamura for the helpful discussion, and Y. Shirakiya and N. Mukai for the excellent technical support.

AUTHOR CONTRIBUTIONS

T.F. conceived the idea for this project, designed all experiments and wrote the manuscript. H.K., Y.W. and Y.H. performed all laboratory experiments and H.K., T.K. and Y.W. performed all animal experiments. S.K. provided crucial ideas and helped with data interpretation. T.F., F.U., F.T. and N.T. provided technical assistance. S.K. provided the hTERT promoter. H.M. constructed the OBP-401 virus. Y.U. developed a protocol for virus manufacture and validation.

COMPETING INTERESTS STATEMENT

The authors declare competing financial interests (see the *Nature Medicine* website for details).

Published online at http://www.nature.com/naturemedicine/
Reprints and permissions information is available online at http://npg.nature.com/reprintsandpermissions/

1. Tearney, G.J. *et al.* *In vivo* endoscopic optical biopsy with optical coherence tomography. *Science* **276**, 2037–2039 (1997).
2. MacDonald, S.L. & Hansell, D.M. Staging of non-small cell lung cancer: imaging of intrathoracic disease. *Eur. J. Radiol.* **45**, 18–30 (2003).
3. Kelloff, G.J. *et al.* Progress and promise of FDG-PET imaging for cancer patient management and oncologic drug development. *Clin. Cancer Res.* 11, 2785–2808 (2005).
4. McMasters, K.M. *et al.* Sentinel lymph node biopsy for melanoma: controversy despite widespread agreement. *J. Clin. Oncol.* **19**, 2851–2855 (2001).
5. Kuerer, H.M. & Newman, L.A. Lymphatic mapping and sentinel lymph node biopsy for breast cancer: developments and resolving controversies. *J. Clin. Oncol.* **23**, 1698–1705 (2005).
6. Koopal, S.A. *et al.* Frozen section analysis of sentinel lymph nodes in melanoma patients. *Cancer* **89**, 1720–1725 (2000).
7. Tanis, P.J. *et al.* Frozen section investigation of the sentinel node in malignant melanoma and breast cancer. *Ann. Surg. Oncol.* **8**, 222–226 (2001).
8. Gulec, S.A., Su, J., O'Leary, J.P. & Stolier, A. Clinical utility of frozen section in sentinel node biopsy in breast cancer. *Am. Surg.* **67**, 529–532 (2001).
9. Chao, C. *et al.* Utility of intraoperative frozen section analysis of sentinel lymph nodes in breast cancer. *Am. J. Surg.* **182**, 609–615 (2001).
10. Misteli, T. & Spector, D.L. Applications of the green fluorescent protein in cell biology and biotechnology. *Nat. Biotechnol.* **15**, 961–964 (1997).
11. van Roessel, P. & Brand, A.H. Imaging into the future: visualizing gene expression and protein interactions with fluorescent proteins. *Nat. Cell Biol.* **4**, E15–E20 (2002).
12. Ehrhardt, D. GFP technology for live cell imaging. *Curr. Opin. Plant Biol.* **6**, 622–628 (2003).
13. Yang, M., Baranov, E., Moossa, A.R., Penman, S. & Hoffman, R.M. Visualizing gene expression by whole-body fluorescence imaging. *Proc. Natl Acad. Sci. USA* **97**, 12278–12282 (2000).
14. Hasegawa, S. *et al.* *In vivo* tumor delivery of the green fluorescent protein gene to report future occurrence of metastasis. *Cancer Gene Ther.* **7**, 1336–1340 (2000).
15. Ohtani, S. *et al.* Quantitative analysis of p53-targeted gene expression and visualization of p53 transcriptional activity following intratumoral administration of adenoviral p53 *in vivo*. *Mol. Cancer Ther.* **3**, 93–100 (2004).
16. Kawashima, T. *et al.* Telomerase-specific replication-selective virotherapy for human cancer. *Clin. Cancer Res.* **10**, 285–292 (2004).
17. Taki, M. *et al.* Enhanced oncolysis by a tropism-modified telomerase-specific replication selective adenoviral agent OBP-405 ("Telomelysin-RGD"). *Oncogene* **24**, 3130–3140 (2005).
18. Umeoka, T. *et al.* Visualization of intrathoracically disseminated solid tumors in mice with optical imaging by telomerase-specific amplification of transferred green fluorescent protein gene. *Cancer Res.* **64**, 6259–6265 (2004).
19. Gu, J., Andreeff, M., Roth, J.A. & Fang, B. hTERT promoter induces tumor-specific Bax gene expression and cell killing in syngenic mouse tumor model and prevents systemic toxicity. *Gene Ther.* **9**, 30–37 (2002).
20. Tsutsumi, S., Kuwano, H., Morinaga, N., Shimura, T. & Asao, T. Animal model of para-aortic lymph node metastasis. *Cancer Lett.* **169**, 77–85 (2001).
21. Maehara, Y. *et al.* Clinical significance of occult micrometastasis in lymph nodes from patients with early gastric cancer who died of recurrence. *Surgery* **119**, 397–402 (1996).
22. Coello, M.C., Luketich, J.D., Litle, V.R. & Godfrey, T.E. Prognostic significance of micrometastasis in non-small-cell lung cancer. *Clin. Lung Cancer* **5**, 214–225 (2004).
23. Fujiwara, T. *et al.* Multicenter phase I study of repeated intratumoral delivery of adenoviral p53 (ADVEXIN) in patients with advanced non-small cell lung cancer. *J. Clin. Oncol.* **24**, 1689–1699 (2006).
24. Hiyama, K. *et al.* Activation of telomerase in human lymphocytes and hematopoietic progenitor cells. *J. Immunol.* **155**, 3711–3715 (1995).
25. Adams, J.Y. *et al.* Visualization of advanced human prostate cancer lesions in living mice by a targeted gene transfer vector and optical imaging. *Nat. Med.* **8**, 891–897 (2002).
26. Yang, M., Luiken, G., Baranov, E. & Hoffman, R.M. Facile whole-body imaging of internal fluorescent tumors in mice with an LED flashlight. *Biotechniques* **39**, 170–172 (2005).
27. Watanabe, T. *et al.* Histone deacetylase inhibitor FR901228 enhances the antitumor effect of telomerase-specific replication-selective adenoviral agent OBP-301 in human lung cancer cells. *Exp. Cell Res.* **312**, 256–265 (2006).
28. Fujiwara, T. *et al.* Enhanced antitumor efficacy of telomerase-selective oncolytic adenoviral agent OBP-401 with docetaxel: preclinical evaluation of chemovirotherapy. *Int. J. Cancer* **119**, 432–440 (2006).

Impact of Convective Flow on the Cellular Uptake and Transfection Activity of Lipoplex and Adenovirus

Takahiro FUJIWARA,[a,b] Hidetaka AKITA,[a,b] Katsuko FURUKAWA,[c] Takashi USHIDA,[c] Hiroyuki MIZUGUCHI,[d] and Hideyoshi HARASHIMA*[,a,b]

[a] *Graduate School of Pharmaceutical Sciences, Hokkaido University; Sapporo, Hokkaido 060–0812, Japan:* [b] *CREST, Japan Science and Technology Corporation (JST); Japan:* [c] *Graduate School of Engineering, University of Tokyo; Tokyo, 113–8656, Japan: and* [d] *Pharmaceuticals and Medical Devices Agency; Tokyo 100–0013, Japan.*

Received March 7, 2006; accepted April 5, 2006; published online April 11, 2006

An *in vitro* cell culture model that mimics *in vivo* extracellular environment would be useful in developing in vivo gene delivery system. In the present study, a parallel flow model was applied to investigate the impact of convective flow on cellular uptake and transfection activity in endothelial cells. LipofectAMINE PLUS and adenovirus were used as model vectors, which bind cells *via* electrostatic- and ligand-receptor interactions, respectively. Whereas a convective flow increased the total amount of vector passing through the flow chamber by 3 orders of magnitude, uptake was increased by less than 10-fold, suggesting that the flow severely inhibited cellular uptake by reducing the retention time in the chamber and/or by diminishing the affinity between the cell and vector. Moreover, the uptake of both vectors was increased in a shear stress-dependent manner to a comparable extent, suggesting that the effect of flow on the cellular uptake was not significant. In contrast, transfection efficiency (TE), expressed as the transfection activity normalized by the cellular uptake of vectors was dramatically stimulated by shear stress, only when LipofectAMINE PLUS was used. Since the activities of the CMV promoter were unaffected by a shear stress, it is possible that altered intracellular trafficking may responsible for the improvement in lipoplex-mediated TE, presumably related to the cellular uptake pathway.

Key words convective flow; gene delivery; adenovirus; lipoplex

The targeting of therapeutic genes to various organs *via* systemic administration is an ideal concept for non-invasive gene therapy in curing malignant diseases. To realize a sophisticated gene delivery system, efforts have been made to develop viral and non-viral vectors. As a result, certain types of transfection tools such as lipoplexes, polyplexes and adenoviruses are currently available, which can exhibit a high transfection activity for *in vitro* cultured cells. However, even when non-viral vectors and adenovirus vectors are administered to the systemic circulation *in vivo*, the transfection activities are exclusively limited to the lung[1—4] and liver,[5,6] respectively. In the case of lipoplexes and polyplexes, they immediately form large aggregates with erythrocytes,[1—4] and then rapidly accumulate in the lung.[7,8] Similarly, the transgene expression of adenovirus is exclusively limited to the liver after an i.v. administration of adenovirus mainly due to the high hepatic clearance[5,9,10] *via* multiple binding between hepatic cells and adenovirus[5,6] (*e.g.* CAR-fiber, integrin-RGD motif and fiber shaft-heparan sulfate interactions).

However, considering that blood flow rate in an artery (5.6 l/min in human[11] and *ca.* 460 ml/min in guinea pig[12]) and blood volume (*ca.* 5.4 l in 70 kg human body weight[13] and *ca.* 200 ml in 2.3 kg guinea pig bogy weight[12]), gene vectors are calculated to be pumped out and back to the heart within approximately 1 min. In other words, gene vectors are able to pass through various organs many times before their elimination from the systemic circulation. This is inconsistent with the fact that transgene expression is barely detectable in organs such as the heart, kidney and muscle except for the lung or liver.

The discrepancy between *in vivo* and *in vitro* transfection activity can be attributed to differences in the extracellular environments of the target cells. One factor that has been clearly identified is plasma protein. When vectors are administered to the systemic circulation, many types of plasma proteins, including lipoproteins, bind to the vectors, resulting in a drastic loss in transfection efficiency.[14,15] On the other hand, in a typical *in vitro* transfection, vectors are applied using serum-free culture medium. Another factor that may affect the *in vivo* transfection activity is blood flow. Since current *in vitro* transfection studies have been carried out under static condition, it is difficult to estimate the effect of fluid flow on transfection activity. Two possible effects are possible; namely, physical effect and biological effect. In the former case, convective flow would wash out the vectors before they reach the cellular surface by sedimentation, and /or it may affect an intrinsic affinity constant for the association between vector and cell. In the latter case, certain types of mechano-sensors (*e.g.* receptor tyrosine kinases[16]), signaling pathways (*e.g.* protein kinase C[17]) and the expression of endogenous genes (*e.g.* platelet-derived growth factor[18,19]) could affect a response to shear stress, which is generally loaded at a border of cellular surface and convective flow in horizontal direction.[20] Since transfection activity is highly dependent on intracellular trafficking and intranuclear transcription,[21—23] shear stress may change the transfection efficiency of transgenes that are taken up by cells.

In the present study, we investigate the influence of convective flow on cellular uptake and transfection activity by means of a parallel flow model. For a comparison, lipoplex and adenovirus vectors which are taken up *via* absorptive- and receptor-mediated endocytosis, respectively, were used in an attempt to clarify the uptake mechanism-dependent influence of flow on transfection activity from physical and biological points of view.

* To whom correspondence should be addressed. e-mail: harasima@pharm.hokudai.ac.jp

MATERIALS AND METHODS

Materials MBEC4 cells derived from mouse brain endothelial cells were generously supplied by Dr. T. Tsuruo and Dr. M. Naito (Tokyo University, Japan). The cells were maintained in DMEM supplemented with 10% fetal bovine serum and 0.5 μg/ml heparin sulfate under an atmosphare of 5% CO_2/air at 37 °C. To prepare the reporter gene vector for the pDNA (pcDNA3.1-GL3), an insert fragment encoding luciferase (GL3) was obtained by HindIII/XbaI digestion of the pGL3-basic vector (Promega, Madison, WI, U.S.A.), and ligated to the HindIII/XbaI digested site of the pcDNA3.1 (Invitrogen Corp, Carlsbad, CA, U.S.A.). LipofectAMINE PLUS was obtained from the Invitrogen Corp. All other chemicals used were commercially available and were reagent grade. Concerning the viral vector, the E_1^-, E_3^-, a replication-deficient serotype 5 adenovirus in which an expression cassette was inserted in the E_1 position was used.[24] In addition, an RGD peptide was inserted in the HI loop of the fiber knob to improve transfection activity to the mouse-derived cells.[25] The expression cassette consisted of a cytomegalovirus promoter/enhancer, cDNA encoding luciferase (GL3) and BGH polyadenylation sequences which were also encoded in the pDNA used in the LipofectAMINE PLUS-mediated transfection.

Parallel Flow Device A parallel flow model was established, as described in a previous study with minor modifications.[26,27] A rectangular channel (14×4 mm^2) was compartmentalized by silicon films (0.3 mm height) on the slide slips (Matsunami, Osaka, Japan), and 2×10^4 cells were then seeded on the channel after coating with laminin, and the cells were then cultured for 40 h until reaching confluence. Slides were mounted on the chamber as illustrated in Fig. 1. The flow loop, reservoirs and infusion pump (Pharmacia, LKB·Pump P500) were perfused with Krebs-Ringer bicarbonate buffer (4.8 mM KCl, 1.0 mM KH_2PO_4, 1.2 mM $MgSO_4$, 1.5 mM $CaCl_2$, 120 mM $NaCl_2$, 24 mM $NaHCO_3$, 12.5 mM HEPES, 5.0 mM Glucose: pH 7.4) containing 8.0 μg DNA/30 ml of lipoplex or 1.0×10^9 particle titer/30 ml of adenovirus. The upstream flow loop was then connected to the inlet port to allow the perfusate flow in the chamber. The fluid flow from the chamber outlet port was recovered in the reservoir and the medium was recirculated throughout the transfection experiments. To maintain the temperature of the perfusate passing through the flow chamber at 37 °C, the upstream flow loop was temporarily warmed up by water bath at 41—42 °C. The shear stresses (τ) were adjusted to 2.3 and 9.7 dyn/cm^2 by controlling the flow rate (Q) so as to mimic the characteristics of *in vivo* cardiovasculature and veneous, respectively[27] based on the following equation:

$$\tau = \frac{6Q\mu}{bh^2}$$

where μ, b and h denote the viscosity of the fluid perfusate, channel width (0.4 cm) and channel hight (0.03 cm), respectively. The flow chamber positioned vertically during the purfusion.

As a control, cells were incubated with 16.8 μl of Krebs-Ringer buffer containing adenovirus and LipofectAMINE PLUS under static conditions, in which the concentration of vectors and fluid volume in the chamber was adjusted to that used in the perfusion study. To avoid a drying, cells were incubated in humid box. In the perfusion experiment, 8.7 and 35.6 μg of pDNA, and 1.1×10^9 and 4.5×10^9 particles of adenovirus was passed through the parallel flow chamber at 2.3 dyn/cm^2 and 9.7 dyn/cm^2, respectively. As a static control, we adjusted the concentration of the vector to the flow conditions (4.9 ng of pDNA and 5.6×10^5 particle titer of adenovirus in 16.8 μl Krebs-Ringer buffer) since adjustment of the total dose to the flow conditions led to a highly toxic effect.

Quantification of Cellular Uptake of Exogenous DNA pDNA was quantified as demonstrated previously by means of real-time PCR.[23] After incubation with LipofectAMINE PLUS and adenovirus for 30 min, the cells were treated with trypsin to detach them from the slide slip. For quantification of the cellular luciferase genes, plasmid DNA and adenovirus genome DNA was purified from cell lysates by means of a GenElute Mammalian Genome DNA Miniprep kit (Sigma-Aldrich, St. Louis, MO, U.S.A.), and subjected to TaqMan PCR with an ABI PRISM® 7700 Sequence Detection System. The sequence of the probe was 5′-CCGCTGAATTGGAATCCATCTTGCTC-3′ with FAM as a fluorescent dye on the 5′ end and TAMRA as a fluorescence quencher dye labeled to the 3′ end. This probe is designed to anneal to the target between the sense primer (5′-TTGACCGCCT-

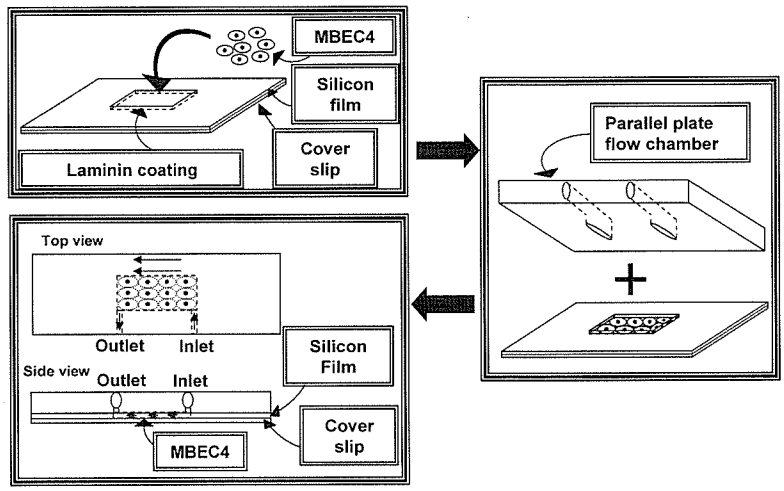

Fig. 1. Schematic Diagram Illustrating the Parallel Flow Model

GAAGTCTCTGA-3′) and the antisense primer (5′-ACACCTGCGTCGAAGATGTTG-3′) in the luciferase sequence. As a reference, a dilution series of pDNA3.1-GL3 was run along with the virus sample.

Transfection Activity After perfusion of the lipoplex and adenovirus for 30 min, the slide slip was transferred to the cell culture dish, and incubated in the culture medium for a further 6 h. The cells were then washed, and lysed with reporter lysis buffer (Promega, Madison, WI, U.S.A.). Luciferase activity was initiated by the addition of 50 μl of luciferase assay reagent (Promega) to 20 μl of cell lysate, and measured by means of a luminometer (Luminescencer-PSN, ATTO, Japan). The amount of protein in the cell lysates was determined using a BCA protein assay kit (PIERCE, Rockford, IL, U.S.A.).

To establish stably transfected MBEC4 cells expressing CMV-driven luciferase, luciferase (GL3)-encoding pcDNA3.1 was transfected into MBEC4 cells by LipofectAMINE PLUS and selected by treatment with 800 μg/ml of G418 for two weeks. The luciferase-positive cell population was maintained in the growth media with 400 μg/ml of G418.

RESULTS AND DISCUSSION

The effect of a convective flow on transfection activity was compared between adenovirus and lipoplex from both physical and biological points of view. Concerning the physical effect, the cellular uptake of lipoplex and adenovirus vector was compared between static and flow conditions. Since physicochemical characters such as size and density are distinct from each other, the velocity of sedimentation (Vs_{ed}) should be also different following Stokes' equation. When a perfusion study is carried out using horizontally seeded cells, cellular uptake may be also affected by the amount of vector, which can sediment on the cell surface during convection through the chamber.[27] To avoid the effect of different sedimentation efficiencies, cell cultures were positioned vertically in the perfusion study.

After perfusion for 30 min, cells were collected to quantify cellular uptake by means of real-time PCR (Fig. 2). Cellular uptake is represented as the percent of the control. As a result, the cellular uptake of adenovirus was increased by 1.2-fold and 3.5-fold by convective flow at 2.3 dyn/cm^2 and 9.7 dyn/cm^2, respectively, compared with static conditions (Fig. 2A). Similarly, the uptake of LipofectAMINE PLUS was also increased by 1.9-fold and 5.8-fold, respectively (Fig. 2B). Cellular uptake was enhanced by stimulating the cellular association of the vector due to fluid motion and by the increased amount of dose passing through the flow chamber. Furthermore, cellular uptake was enhanced to the same extent (approximately 3-folds) when the flow rate was increased from 2.3 to 9.7 dyn/cm^2 for both vectors, indicating that the impact of flow on cellular uptake between LipofectAMINE PLUS and adenovirus was not significant. The enhancement in cellular uptake (less than 10 fold) was much less prominent than that for the dose passing through the chamber (1935-fold and 7946-fold higher than static conditions at 2.3 dyn/cm^2 and 9.7 dyn/cm^2, respectively). This suggests that the collision of vectors with the cellular surface is severely perturbed by convective flow since unbound vectors gaining access to the cellular surface were washed out and/or

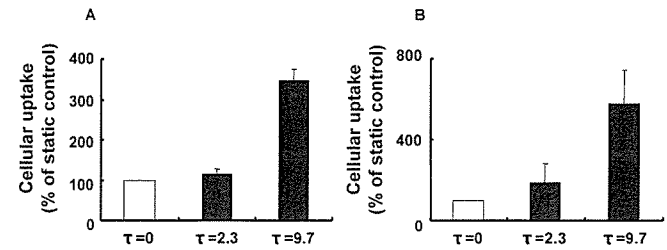

Fig. 2. Effect of Convective Flow on the Cellular Uptake of Adenovirus (A) and LipofectAMINE PLUS (B)

Adenovirus (A) and LipofectAMINE PLUS (B) was perfused with Krebs-Ringer bicarbonate containing 8.0 μg DNA/30 ml of lipoplex or 1.0×10^9 particle titer/30 ml of adenovirus for 30 min. As a control, cells were incubated with 16.8 μl of Krebs-Ringer buffer containing adenovirus and LipofectAMINE PLUS under static conditions, in which the concentration of vector and fluid volumes in the chamber were adjusted to the perfusion study. Cellular uptake was quantified by means of TaqMan PCR. Cellular uptake is represented as percent of static condition. Each bar represent the mean and standard deviation of three experiments.

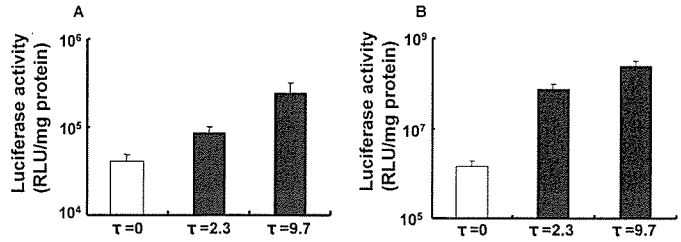

Fig. 3. Effect of Convective Flow on the Transfection Activity of Adenovirus (A) and LipofectAMINE PLUS (B)

Cells were incubated with adenovirus (A) and LipofectAMINE PLUS (B) under static and shear stress conditions for 30 min. Cells were further incubated in cell culture medium for an additional 6 h. Transgene expression was evaluated by luciferase activity. Each bar represent the mean and standard deviation of three experiments.

the affinity between vector and cell surface was decreased.

As shown in Fig. 2B, the cellular uptake of the lipoplex increased monotonically depending on the shear stress. This is inconsistent with a previous observation reporting that cellular uptake was temporary increased at 2.3 dyn/cm^2 and then decreased when the stress was further increased to 9.7 dyn/cm^2.[27] The overall influence of shear stress on the cellular uptake is balanced by a stimulative effect which induces collisions between vectors and cells, and by a negative effect which prevents the association and/or enhances the dissociation between cells and vectors[28] by its hydrodynamic force. This discrepancy can be accounted for by assuming that the cellular binding of LipofectAMINE PLUS is stronger than that of TransIT (Panvela) which was used in the previous study.[27]

The biological effect of shear stress was investigated by measuring transfection activity. In adenovirus, transgene expression was stimulated by a convective flow by 2.1 times and 5.9 times at 2.3 dyn/cm^2 and 9.7 dyn/cm^2, respectively compared with static conditions (Fig. 3A). Transfection efficiency (TE) calculated as transfection activity normalized by the cellular uptake of adenovirus is summarized in Table 1. TE values are quite comparable values regardless of the extent of shear stress. This indicates that the transfection activity is directly related to the cellular uptake of adenoviral DNA under the flow conditions. In contrast, the transgene expression of LipofectAMINE PLUS was drastically increased by 53 times at 2.3 dyn/cm^2 (Fig. 3B), whereas cellular uptake was increased by only 1.9 times (Fig. 2B). As a result, the TE

Table 1. Cellular Uptake, Transfection Activity, and Transfection Efficiency (TE) (% of Static Control)

	Cellular uptake (A) (% of static control)	Transfection activity (B) (% of static control)	TE (B/A)
Adenovirus (τ=2.3)	116±12	212±31	1.83
Adenovirus (τ=9.7)	349±27	588±180	1.68
LipofectAMINE PLUS (τ=2.3)	190±90	5330±1590	28.1
LipofectAMINE PLUS (τ=9.7)	576±166	17800±4630	30.9

The cellular uptake is measured by real-time PCR. The transfection activity is measured by luciferase assay and protein assay. TE is calculated by dividing B by A.

value at 2.3 dyn/cm^2 was calculated to be 28 times higher than that under static conditions, as summarized in the Table 1. This suggests that TE of pDNA taken up by the cells were stimulated by a shear stress. In contrast to the differences between static conditions and low shear stress conditions (2.3 dyn/cm^2), the TE values were quite comparable, regardless of the extent of shear stress (2.3 dyn/cm^2 and 9.7 dyn/cm^2). Therefore, a low shear stress was sufficient to trigger a certain types of intracellular mechanism related to increasing TE.

It is possible that the drastic improvement in TE by shear stress in Lipoplex-mediated transfection is due to the stimulation of the activity of the CMV promoter, since previous reports showed that expression level of endogenous genes was altered under conditions of shear stress.[19] The intrinsic activities of endogenous transcription factors associated with the CMV promoter were compared between static and shear stress conditions by measuring the luciferase activity of stable transfectants, expressing CMV-driven luciferase-encoding pDNA (pcDNA3.1-Luc). As a result, the stable transfectant exhibited a comparable luciferase activity (Fig. 4), suggesting that the intrinsic activity of transcription factors is not affected by shear stress. Intracellular trafficking is more susceptible to be responsible for the improvement in TE compared with intranuclear transcription process.

The mechanism underlying the lipoplex-specific increase in TE is illustrated in Fig. 5. Previous studies showed that shear stress induced the production of intracellular signaling-related proteins such protein kinase C,[17] MAP kinase[29] and Rho GTPases,[30] which control the various clathrin-independent pathways such as pinocytosis[31] and phagocytosis.[32] In the case of adenovirus, binding is based on specific ligand-receptor interactions between the fiber proteins and coxsackievirus and the adenovirus receptor (CAR), and between the RGD motif in the penton base and integrin.[33] Thus, it is plausible that the cellular uptake pathway of adenovirus is limited to the receptor-mediated endocytosis. In contrast, plasmid DNA condensed with LipofectAMINE PLUS is able to bind to the entire cell surface area *via* electrostatic interactions. If novel pathway was stimulated by shear stress, lipoplex could then internalize *via* alternative pathways, in addition to classical endocytosis. Currently, we have clarified that transfection activity is closely related to the cellular uptake pathway, which determines intracellular fate. It should be noted that gene vector taken up *via* macropinocytosis can avoid the lysosomal degradation, and resulted in the high transfection activity.[34] Therefore, it is possible that shear stress may alter the cellular uptake route of a lipoplex, which is advantageous for the transgene-expression.

Collectively, impact of convective flow on cellular uptake and transfection activity was investigated with LipofectAMINE PLUS and adenovirus as models, which interact with cells *via* electrostatic and ligand-receptor interactions, respectively. Regarding the cellular uptake process, convective flow severely perturbed the cellular uptake of both vectors to the same extent by washing out the vector from the chamber before they reached cellular surface, and/or reducing the

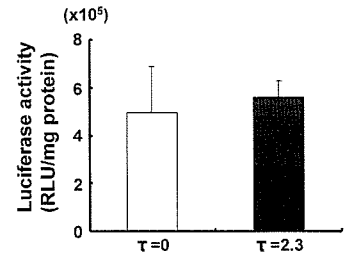

Fig. 4. Effect of Convective Flow on the Intrinsic Activity of Transcription Factors for the CMV Promoter

MBEC4 cells stably expressing luciferase were seeded on the parallel flow chamber. Luciferase activity was measured before and after the exposure to convective flow at 2.3 dyn/cm^2 for 30 min. Each bar represents the mean and standard deviation of three experiments.

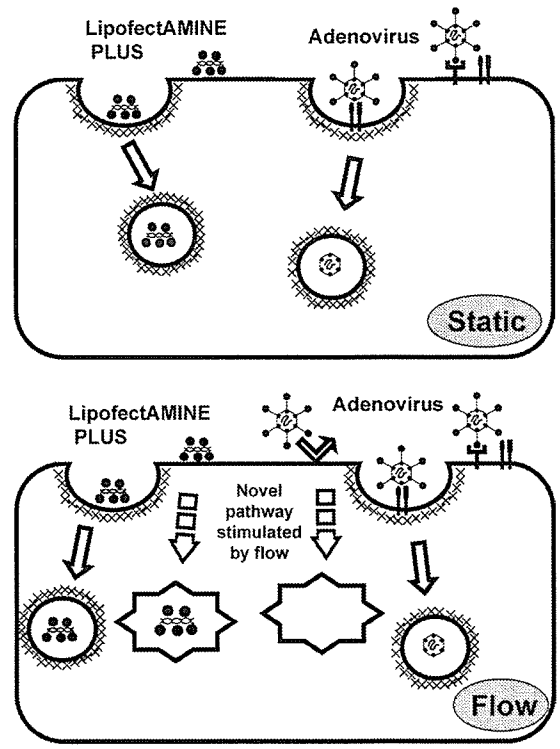

Fig. 5. Schematic Diagram Illustrating the Possible Cellular Uptake Pathways of Adenovirus and LipofectAMINE PLUS Under the Static and Flow Condition

affinity between the vector and the cellular surface. In contrast, transfection efficiency, denoted as transfection activity normalized by the cellular uptake of exogenous DNA, was drastically stimulated by shear stress only in the case of LipofectAMINE PLUS. Considering that the intrinsic activities of endogenous transcription factors associated with the CMV promoter were unaffected by shear stress, it is possible that intracellular trafficking, presumably linked to the cellular uptake mechanism, may be responsible for the improved lipoplex-mediated transfection.

This is the first demonstration, in which the effects of convective flow on the cellular uptake and transfection activity have been assessed separately. Further studies with other cell lines derived from endothelial cells (*e.g.* HUVEC) are valuable to lead a generality of this phenomenon. This model system will be useful for developing a flow-resistance to gene delivery system.

Acknowledgements This work was supported in part by Grants-in-Aid for Scientific Research (B) and Grant-in-Aid for Young Scientists (B) from the Ministry of Education, Culture, Sports, Science and Technology of Japan, and by Grants-in-Aid for Scientific Research on Priority Areas from the Japan Society for the Promotion of Science.

REFERENCES

1) Kircheis R., Wightman L., Schreiber A., Robitza B., Rossler V., Kursa M., Wagner E., *Gene Ther.*, **8**, 28—40 (2001).
2) Ogris M., Brunner S., Schuller S., Kircheis R., Wagner E., *Gene Ther.*, **6**, 595—605 (1999).
3) Sakurai F., Nishioka T., Yamashita F., Takakura Y., Hashida M., *Eur. J. Pharm. Biopharm.*, **52**, 165—172 (2001).
4) Sakurai F., Nishioka T., Saito H., Baba T., Okuda A., Matsumoto O., Taga T., Yamashita F., Takakura Y., Hashida M., *Gene Ther.*, **8**, 677—686 (2001).
5) Koizumi N., Mizuguchi H., Sakurai F., Yamaguchi T., Watanabe Y., Hayakawa T., *J. Virol.*, **77**, 13062—13072 (2003).
6) Mizuguchi H., Hayakawa T., *Hum. Gene Ther.*, **15**, 1034—1044 (2004).
7) Mahato R. I., Kawabata K., Nomura T., Takakura Y., Hashida M., *J. Pharm. Sci.*, **84**, 1267—1271 (1995).
8) Mahato R. I., Kawabata K., Takakura Y., Hashida M., *J. Drug Target.*, **3**, 149—157 (1995).
9) Lieber A., He C. Y., Meuse L., Schowalter D., Kirillova I., Winther B., Kay M. A., *J. Virol.*, **71**, 8798—8807 (1997).
10) Wolff G., Worgall S., van Rooijen N., Song W. R., Harvey B. G., Crystal R. G., *J. Virol.*, **71**, 624—629 (1997).
11) Benowitz N., Forsyth F. P., Melmon K. L., Rowland M., *Clin. Pharmacol. Ther.*, **16**, 87—98 (1974).
12) Peeters L. L., Grutters G., Martin C. B., Jr., *Am. J. Obstet. Gynecol.*, **138**, 1177—1184 (1980).
13) Spector W. S., "Handbook of Biological Data," W. B. Saunders, Philadelohia, 1956.
14) Tandia B. M., Vandenbranden M., Wattiez R., Lakhdar Z., Ruysschaert J. M., Elouahabi A., *Mol. Ther.*, **8**, 264—273 (2003).
15) Tandia B. M., Lonez C., Vandenbranden M., Ruysschaert J. M., Elouahabi A., *J. Biol. Chem.*, **280**, 12255—12261 (2005).
16) Chen K. D., Li Y. S., Kim M., Li S., Yuan S., Chien S., Shyy J. Y., *J. Biol. Chem.*, **274**, 18393—18400 (1999).
17) Hu Y. L., Chien S., *J. Histochem. Cytochem.*, **45**, 237—249 (1997).
18) Hsieh H. J., Li N. Q., Frangos J. A., *Am. J. Physiol.*, **260**, H642—646 (1991).
19) Resnick N., Collins T., Atkinson W., Bonthron D. T., Dewey C. F., Jr., Gimbrone M. A., Jr., *Proc. Natl. Acad. Sci. U.S.A.*, **90**, 4591—4595 (1993).
20) Li Y. S., Haga J. H., Chien S., *J. Biomech.*, **38**, 1949—1971 (2005).
21) Kamiya H., Akita H., Harashima H., *Drug Discov. Today*, **8**, 990—996 (2003).
22) Akita H., Ito R., Khalil I. A., Futaki S., Harashima H., *Mol. Ther.*, **9**, 443—451 (2004).
23) Hama S., Akita H., Ito R., Mizuguchi H., Hayakawa T., Harashima H., *Mol. Ther.*, **13**, 786—794 (2006).
24) Mizuguchi H., Kay M. A., Hayakawa T., *Biotechniques*, **30**, 1112—1114, 1116 (2001).
25) Koizumi N., Mizuguchi H., Hosono T., Ishii-Watabe A., Uchida E., Utoguchi N., Watanabe Y., Hayakawa T., *Biochim. Biophys. Acta*, **1568**, 13—20 (2001).
26) Levesque M. J., Nerem R. M., *J. Biomech. Eng.*, **107**, 341—347 (1985).
27) Harris S. S., Giorgio T. D., *Gene Ther.*, **12**, 512—520 (2005).
28) Wattenbarger M. R., Graves D. J., Lauffenburger D. A., *Biophys. J.*, **57**, 765—777 (1990).
29) Sumpio B. E., Yun S., Cordova A. C., Haga M., Zhang J., Koh Y., Madri J. A., *J. Biol. Chem.*, **280**, 11185—11191 (2005).
30) Li S., Chen B. P., Azuma N., Hu Y. L., Wu S. Z., Sumpio B. E., Shyy J. Y., Chien S., *J. Clin. Invest.*, **103**, 1141—1150 (1999).
31) Mace G., Miaczynska M., Zerial M., Nebreda A. R., *Embo. J.*, **24**, 3235—3246 (2005).
32) Niedergang F., Chavrier P., *Curr. Top. Microbiol. Immunol.*, **291**, 43—60 (2005).
33) Meier O., Boucke K., Hammer S. V., Keller S., Stidwill R. P., Hemmi S., Greber U. F., *J. Cell Biol.*, **158**, 1119—1131 (2002).
34) Khalil I. A., Kogure K., Futaki S., Harashima H., *J. Biol. Chem.*, in press,

Efficient Gene Transfer into Differentiated Human Trophoblast Cells with Adenovirus Vector Containing RGD Motif in the Fiber Protein

Naoya KOIZUMI,[a,c] Hiroyuki MIZUGUCHI,[a,b] Masuo KONDOH,*[,b,c] Makiko FUJII,[c] Tsuyoshi NAKANISHI,[d] Naoki UTOGUCHI,[e] and Yoshiteru WATANABE[c]

[a] *Laboratory of Gene Transfer and Regulation, National Institute of Biomedical Innovation; Osaka 567–0085, Japan:* [b] *Graduate School of Pharmaceutical Sciences, Osaka University; Osaka 565–0871, Japan:* [c] *Department of Pharmaceutics and Biopharmaceutics, Showa Pharmaceutical University; Tokyo 194–8543, Japan:* [d] *Department of Toxicology, Graduate School of Pharmaceutical Sciences, Osaka University; Osaka 565–0871, Japan: and* [e] *Department of Biopharmaceutics, School of Pharmaceutical Sciences, Teikyo University; Kanagawa 199–0195, Japan.*
Received February 17, 2006; accepted March 10, 2006

Previously we reported fiber-modified adenovirus (Ad) vectors containing the Arg-Gly-Asp (RGD) motif on the HI loop of the fiber knob (Ad-RGD vectors) have high gene transfer efficacy into some human trophoblast cell lines. In the current study, we investigate transgene activity of Ad-RGD during differentiation of human cytotrophoblast BeWo cells into syncytiotrophoblast-like cells. Although cellular differentiation into syncytiotrophoblast cells was followed by a decrease in the coxsackievirus and adenovirus receptor levels on the cell membrane, the $\alpha V\beta 3$ and $\alpha V\beta 5$ integrin levels did not change. Conventional adenovirus vector had lower transduction activity in the differentiated cells than non-differentiated cells. In contrast, Ad-RGD vector had no influence on differentiation and had a *ca.* 2—5 fold higher transduction activity than that of the conventional Ad vector. Thus, Ad-RGD vector can be a powerful tool for gene transfer experiments in syncytiotrophoblast cells.

Key words trophoblast; adenovirus vector; gene transfer

Placenta plays a vital role in fetal growth. There are several types of placental cells, including cytotrophoblast, syncytiotrophoblast, endothelial and epithelial cells. Syncytiotrophoblast cells are differentiated from cytotrophoblast cells and located between the maternal fluid and fetus. These cells are responsible for the transfer of nutrients between the mother and fetus.[1] Thus, in order to provide medical treatment to pregnant women, a clear understanding of the function of these trophoblasts is essential.

There are several methods available to transfer genes to cells, which have been classified mainly as non-viral and viral vectors. Trophoblast gene transfer is useful in order to study the biological functions of the placenta. Recombinant adenovirus (Ad) vector and its derivatives are the most frequently used among basic researchers due to their easy preparation and highly infectious nature.[2] Conventional Ad vectors infect cells by interacting between the Ad fiber and its receptor, coxsackievirus and adenovirus receptor (CAR), on the cell surface.[2] This interaction suggests that cells lacking CAR have a very low infectious efficacy with the Ad vectors.[3—6] To overcome this limitation, several investigators have developed fiber-modified Ad vectors that expand vector tropism.[2] Insertion of Arg-Gly-Asp (RGD) and/or 7-tandem lysine residue motif into the HI loop of the fiber protein provided the Ad vectors with CAR-independent tropism in cells expressing integrin and heparin sulfate on the membrane, respectively.[7—13]

Human trophoblast BeWo cells are typically used to model the human placental barrier since cytotrophoblast cells differentiate into syncytiotrophoblast-like cells by treating BeWo cells with forskolin.[14] We and other investigators found that human trophoblasts seem to regulate transportation of zinc, valproic acid, anti-cancer agents, monocarboxylic cells and trialkyltin compounds using BeWo cells.[15—19] The gene transfer method into BeWo cells is extremely effective enabling further detailed analysis in trophoblast cells. As mentioned above, Ad vectors interact with cells *via* CAR on the cell membrane. Expression of CAR, however, reportedly decreased during differentiation from cytotrophoblast to syncytiotrophoblast,[20] and Ad vectors' transgene activity efficacy was low in the syncytiotrophoblast cells.[21,22]

We have previously reported the fiber-modified Ad vector containing a RGD motif (Ad-RGD vector) was superior to conventional Ad vector and other fiber-modified Ad vectors in BeWo cell transgenic activity.[23] Here we evaluated transgenic activity of Ad-RGD vectors in differentiated syncytiotrophoblast-like BeWo cells.

MATERIALS AND METHODS

Cell Culture BeWo cells (clone b30) were obtained from Dr. Alan Schwarts (Washington University, U.S.A.). BeWo cells were cultured in Dulbecco's modified Eagle's medium (DMEM) supplemented with 10% heat-inactivated fetal bovine serum (FBS), 1% MEM non-essential amino acid solution (Gibco, MD, U.S.A.), 1.6 g/l sodium bicarbonate, 0.584 g/l L-glutamine and 3.5 g/l D-glucose.

Differentiation of BeWo Cells BeWo cell differentiation was performed as described previously.[14] Briefly, forskolin (FK) was dissolved in 20 mM ethanol and cells were cultured with DMEM medium containing 50 μM FK. The medium was exchanged every 24 h and the differentiation of BeWo cells into syncytiotrophoblast-like cells was verified through morphological and biochemical features.[15]

Ad Vector Preparation We used wild-type Ad vector, Ad-LacZ, and the fiber-modified Ad vectors, Ad-RGD-LacZ containing RGD peptide, in the HI loop of the fiber knob.[24—26] The virus particle (VP) titer was calculated according to the methods of Maizel *et al.*[27]

Flow Cytometry To detect the cell membrane expression of human CAR, $\alpha V\beta 3$-integrin and $\alpha V\beta 5$-integrin, cells were labeled with mouse monoclonal antibody RmcB

* To whom correspondence should be addressed. e-mail: masuo@phs.osaka-u.ac.jp

(Upstate Biotechnology, Lake Placid, NY, U.S.A.), mouse monoclonal antibody LM609 (CHEMICON International, Inc., Temecula, CA, U.S.A.) and mouse monoclonal antibody P1F6 (CHEMICON International, Inc.), respectively. The cells were then incubated with fluorescein-labeled secondary antibody (Pharmingen, San Diego, CA, U.S.A.). Labeled cells were analyzed by flow cytometry (FACSCalibur, Becton Dickinson, Tokyo, Japan).

LacZ Assay BeWo cells (5×10^4 cells) were seeded into 24-well plates and treated with vehicle or FK (50 μM) 2 d later. After an additional 3 d incubation period, the cells were transduced with Ad-LacZ or Ad-RGD-LacZ for 1.5 h. Two days later the cells were washed with PBS, fixed with 0.5% glutaraldehyde, and stained with X-gal solution (1.3 mM $MgCl_2$, 15 mM NaCl, 44 mM Hepes, 3 mM potassium ferricyanide, 3 mM potassium ferrocyanide, and 0.05% X-gal solution dissolved in dimethylformamide). LacZ production was quantitatively measured using a Luminescent β-galactosidase detection Kit II (Clontech, Tokyo).

RESULTS AND DISCUSSION

The human trophoblast cell line, BeWo, shares common features with cytotrophoblast cells, and elevation of intracellular cAMP by FK-treatment leads to morphological and biochemical changes of cytotrophoblast-like BeWo cells into syncytiotrophoblast-like cells.[14] Therefore, BeWo cells have been widely used to model the human placenta. Prior to this study, we verified treatment of BeWo cells with FK induced cell–cell fusion and human chorionic gonadotropin, both of which are markers of syncytiotrophoblast-like cells.[15] In this study we first investigated expression of CAR, $\alpha V\beta3$-integrin, and $\alpha V\beta5$-integrin in FK-treated BeWo cells. As shown in Fig. 1, CAR cellular expression decreased from 69.3% to 25.1% during BeWo cell differentiation. In contrast, $\alpha V\beta3$-integrin and $\alpha V\beta5$-integrin levels remained unchanged by FK-treatment. These data indicate that conventional Ad vectors might have low transduction efficacy in FK-treated BeWo cells, since CAR is a primary receptor for Ad vector infection.[2]

Mizuguchi's lab has developed several fiber-modified Ad vectors to expand tropism of conventional Ad vectors, one of which are the Ad-RGD vectors where the RGD-motif is inserted in the HI loop of the fiber protein. The Ad-RGD vectors transduce cells *via* $\alpha V\beta3$-integrin and $\alpha V\beta5$ located on the cell membrane.[12,13] The Ad-RGD vector overcame low transduction efficacy of the conventional Ad vector in CAR-negative cells and was used in tumor-therapy.[28,29] Next we evaluated transduction efficacy of Ad-RGD vectors containing the reporter gene, LacZ. As shown in Figs. 2A and B, Ad-RGD-LacZ had higher transduction activity than that of Ad-LacZ containing wild-type fiber in vehicle- and FK-treated BeWo cells. Infection of Ad-RGD-LacZ with vehicle-treated BeWo cells leads to a 9.4-fold increase in LacZ activity compared to Ad-LacZ-infected cells at 2500 particles/cell. Ad-RGD-LacZ also increased LacZ activity compared to Ad-LacZ in FK-treated BeWo cells (6.6-fold). Although

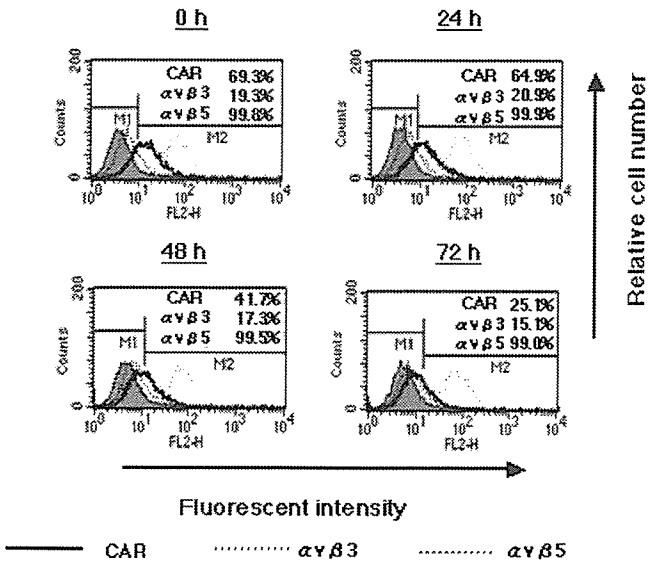

Fig. 1. Flow Cytometric Analysis of CAR, $\alpha V\beta3$-Integrin, and $\alpha V\beta5$-Integrin Expression during BeWo Cell Differentiation

BeWo cells were treated with 50 μM forskolin (FK) for 24—72 h, and the cytotrophoblast-like BeWo cells differentiated into syncytiotrophoblast-like cells under such conditions.[15] The cells were harvested at the indicated periods and then the cells were incubated with anti-CAR, anti-$\alpha V\beta3$-integrin or anti-$\alpha V\beta5$-integrin antibodies, followed by the appropriate fluorescein-labeled secondary antibody. The antibody-bound cells were detected by flow cytometry. Data are representative of two independent experiments.

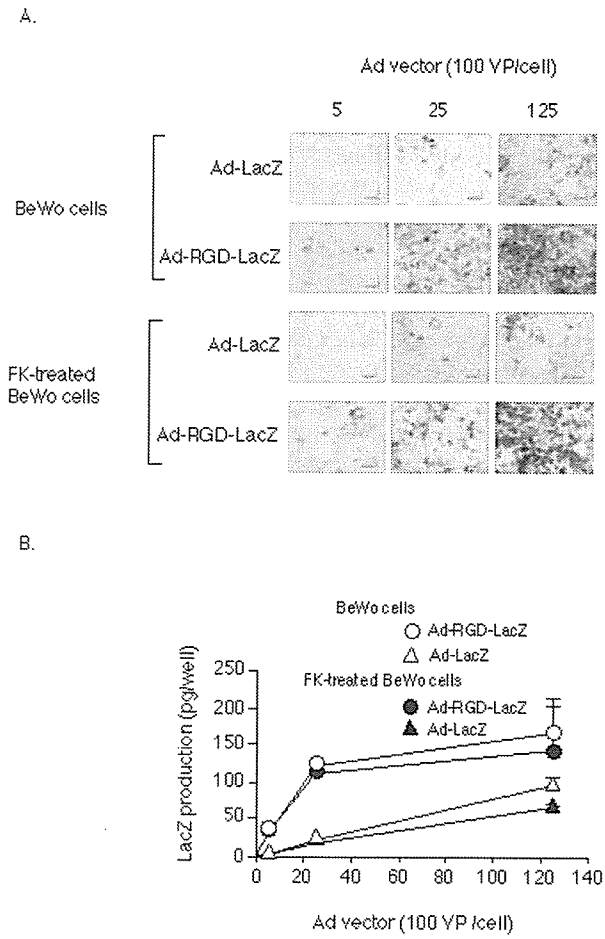

Fig. 2. LacZ Production in Vehicle- or FK-Treated BeWo Cells Transduced by Ad-LacZ or Ad-RGD-LacZ

BeWo cells were treated with vehicle or FK (50 μM) for 72 h. Next, cells were infected with Ad-LacZ or Ad-RGD-LacZ at the indicated concentrations for 1.5 h. After an additional 48 h of culture, X-gal staining was performed (A), and LacZ production was measured (B) as described in the materials and methods. Data are presented as mean±S.D. ($n=3$), from two independent experiments.

Ad-LacZ-mediated LacZ production was decreased to 71% of the vehicle-treated cells in FK-treated cells at 12500 particles/cell, Ad-RGD-LacZ-mediated LacZ production was unaffected by FK treatment. There is discrepancy between reduction of CAR level (from 69.3 to 25.1%) and reduction of LacZ level (71% of the control) in forskolin-treated BeWo cells. CAR level was in partial agreement with CAR-positive cells, but production of LacZ reflected both Ad vector-infected cells and transcriptional activity of expression-cassette in forskolin-treated cells. Ad vectors and Ad-RGD vectors had CMV promoter-driven LacZ gene.[26] Transgene activity of CMV promoter can be augmented by elevated levels of intracellular cyclic AMP.[30,31] Therefore, the discrepancy may be due to activation of CMV promoter by forskolin.

Cellular Ad infection involves two steps. Briefly, the CAR receptor on the cell membrane first interacts with the AB, DE and FG loop of the Ad-fiber knob, and secondly the RGD motif of the Ad-penton base interacts with $\alpha V\beta 3$- and $\alpha V\beta 5$-integrins on the cell membranes followed by the cellular uptake *via* the endocytotic pathway.[3,32—34] The RGD motif inserted into the fiber protein in Ad-RGD-LacZ was located in the HI loop of the fiber knob. It does not play a role in the two step Ad infection, but instead has a high affinity to $\alpha V\beta 3$- and $\alpha V\beta 5$-integrin.[35] Therefore, high transduction efficiency of Ad-RGD vector may be mediated by the ability of the vector to bind both CAR and the $\alpha V\beta 3$- and $\alpha V\beta 5$-integrins in the BeWo cell differentiated model.

There are several vectors, including recombinant herpes simplex virus vector, recombinant adeno-associated virus (AAV) vector, and recombinant sindbis virus vector, used for human trophoblast cell transduction.[22] Among them, the AAV vector can transduce both cytotrophoblast and syncytiotrophoblast cells; however, AAV vector production is difficult.[22] The Ad-RGD vector is easy to prepare and highly capable of transferring genes into both cytotrophoblast and syncytiotrophoblast cells. Thus, Ad-RGD is a promising vector for basic research of human placenta using BeWo cells.

Acknowledgement This work is partly supported by a Grant-in-Aid for Scientific Research from the Ministry of Education, Culture, Sports, Science and Technology, Japan.

REFERENCES

1) Stulc J., *Placenta*, **10**, 113—119 (1989).
2) Mizuguchi H., Hayakawa T., *Hum. Gene Ther.*, **15**, 1034—1044 (2004).
3) Bergelson J. M., Cunningham J. A., Droguett G., Kurt-Jones E. A., Krithivas A., Hong J. S., Horwitz M. S., Crowell R. L., Finberg R. W., *Science*, **275**, 1320—1323 (1997).
4) Miller C. R., Buchsbaum D. J., Reynolds P. N., Douglas J. T., Gillespie G. Y., Mayo M. S., Raben D., Curiel D. T., *Cancer Res.*, **58**, 5738—5748 (1998).
5) Pickles R. J., McCarty D., Matsui H., Hart P. J., Randell S. H., Boucher R. C., *J. Virol.*, **72**, 6014—6023 (1998).
6) Zabner J., Freimuth P., Puga A., Fabrega A., Welsh M. J., *J. Clin. Invest.*, **100**, 1144—1149 (1997).
7) Wickham T. J., Tzeng E., Shears L. L., 2nd, Roelvink P. W., Li Y., Lee G. M., Brough D. E., Lizonova A., Kovesdi I., *J. Virol.*, **71**, 8221—8229 (1997).
8) Dmitriev I., Krasnykh V., Miller C. R., Wang M., Kashentseva E., Mikheeva G., Belousova N., Curiel D. T., *J. Virol.*, **72**, 9706—9713 (1998).
9) Krasnykh V., Dmitriev I., Mikheeva G., Miller C. R., Belousova N., Curiel D. T., *J. Virol.*, **72**, 1844—1852 (1998).
10) Yoshida Y., Sadata A., Zhang W., Saito K., Shinoura N., Hamada H., *Hum. Gene Ther.*, **9**, 2503—2515 (1998).
11) Bouri K., Feero W. G., Myerburg M. M., Wickham T. J., Kovesdi I., Hoffman E. P., Clemens P. R., *Hum. Gene Ther.*, **10**, 1633—1640 (1999).
12) Koizumi N., Mizuguchi H., Hosono T., Ishii-Watabe A., Uchida E., Utoguchi N., Watanabe Y., Hayakawa T., *Biochem. Biophys. Acta*, **1568**, 13—20 (2001).
13) Mizuguchi H., Koizumi N., Hosono T., Utoguchi N., Watanabe Y., Kay M. A., Hayakawa T., *Gene Ther.*, **8**, 730—735 (2001).
14) Wice B., Menton D., Geuze H., Schwartz A. L., *Exp. Cell Res.*, **186**, 306—316 (1990).
15) Asano N., Kondoh M., Ebihara C., Fujii M., Nakanishi T., Utoguchi N., Enomoto S., Tanaka K., Watanabe Y., *Rep. Toxicol.*, **21**, 285—291 (2006).
16) Utoguchi N., Chandorkar G. A., Avery M., Audus K. L., *Reprod. Toxicol.*, **195**, 217—224 (2000).
17) Utoguchi N., Audus K. L., *Int. J. Pharm.*, **14**, 115—124 (2000).
18) Takahashi T., Utoguchi N., Takara A., Yamamoto N., Nakanishi T., Tanaka K., Audus K. L., Watanabe Y., *Placenta*, **22**, 863—869 (2001).
19) Nakanishi T., Kohroki J., Suzuki S., Ishizaki J., Hiromori Y., Takasuga S., Itoh N., Watanabe Y., Utoguchi N., Tanaka K., *J. Clin. Endocrinol. Metab.*, **87**, 2830—2837 (2002).
20) Koi H., Zhang J., Makrigiannakis A., Getsios S., MacCalman C. D., Kopf G. S., Strauss J. F., 3rd, Parry S., *Biol. Reprod.*, **64**, 1001—1009 (2001).
21) MacCalman C. D., Furth E. E., Omigbodun A., Kozarsky K. F., Coutifaris C., Strauss J. F., III, *Biol. Reprod.*, **54**, 682—691 (1996).
22) Parry S., Holder J., Halterman M. W., Weitzman M. D., Davis A. R., Federoff H., Strauss J. F., 3rd., *Am. J. Pathol.*, **152**, 1521—1529 (1998).
23) Koizumi N., Kondoh M., Mizuguchi H., Nakanishi T., Masuyama A., Ida F., Fujii M., Hayakawa T., Nakashima E., Tanaka K., Watanabe Y., *Placenta*, **26**, 729—734 (2005).
24) Mizuguchi H., Kay M. A., *Hum. Gene Ther.*, **9**, 2577—2583 (1998).
25) Mizuguchi H., Kay M. A., *Hum. Gene Ther.*, **10**, 2013—2017 (1999).
26) Okada N., Tsukada Y., Nakagawa S., Mizuguchi H., Mori K., Saito T., Fujita T., Yamamoto A., Hayakawa T., Mayumi T., *Biochem. Biophys. Res. Commun.*, **282**, 173—179 (2001).
27) Maizel J. V., Jr., White D. O., Scharff M. D., *Virology*, **36**, 115—125 (1968).
28) Okada N., Saito T., Masunaga Y., Tsukada Y., Nakagawa S., Mizuguchi H., Mori K., Okada Y., Fujita T., Hayakawa T., Mayumi T., Yamamoto A., *Cancer Res.*, **61**, 7913—7919 (2001).
29) Okada N., Iiyama S., Okada Y., Mizuguchi H., Hayakawa T., Nakagawa S., Mayumi T., Fujita T., Yamamoto A., *Cancer Gene Ther.*, **12**, 72—83 (2005).
30) Stamminger T., Fickenscher H., Fleckenstein B., *J. Gen. Virol.*, **71**, 105—113 (1990).
31) Wilkinson G. W., Akrigg A., *Nucleic Acids Res.*, **20**, 2233—2239 (1992).
32) Bergelson J. M., Krithivas A., Celi L., Droguett G., Horwitz M. S., Wickham T., Crowell R. L., Finberg R. W., *J. Virol.*, **72**, 415—419 (1998).
33) Tomko R. P., Xu R., Philipson L., *Proc. Natl. Acad. Sci. U.S.A.*, **94**, 3352—3356 (1997).
34) Wickham T. J., Filardo E. J., Cheresh D. A., Nemerow G. R., *J. Cell Biol.*, **127**, 257—264 (1994).
35) Koivunen E., Wang B., Ruoslahti E., *Biotechnology*, **13**, 265—270 (1995).

Highlighted paper selected by Editor-in-chief

Non-Methylated CpG Motif Packaged into Fusogenic Liposomes Enhance Antigen-Specific Immunity in Mice

Tomoaki YOSHIKAWA,[a,b] Susumu IMAZU,[a] Jian-Qing GAO,[a,c] Kazuyuki HAYASHI,[a] Yasuhiro TSUDA,[a] Naoki OKADA,[a,d] Yasuo TSUTSUMI,[e] Mitsuru AKASHI,[b,f] Tadanori MAYUMI,[g] and Shinsaku NAKAGAWA*[,a,b]

[a] *Department of Biopharmaceutics, Graduate School of Pharmaceutical Sciences, Osaka University; 1–6 Yamadaoka, Suita, Osaka 565–0871, Japan:* [b] *"Creation of bio-devices and bio-systems with chemical and biological molecules for medical use", CREST, Japan Science and Technology Agency (JST); Tokyo 102–8666, Japan:* [c] *Department of Pharmaceutics, College of Pharmaceutical Sciences, Zhejiang University; 353 Yan-an Road, Hangzhou 310031, P.R. China:* [d] *Department of Biopharmaceutics, Kyoto Pharmaceutical University; 5 Nakauchi-cho, Misasagi, Yamashina-ku, Kyoto 607–8414, Japan:* [e] *National Institute of Biomedical Innovation; 7–6–8 Saito-Asagi, Ibaraki, Osaka 567–0085, Japan:* [f] *Department of Molecular Chemistry, Graduate School of Engineering, Osaka University; 2–1 Yamadaoka, Suita 565–0871, Japan: and* [g] *Kobegakuin University; 518 Arise, Ikawadani-cho, Nishi-ku, Kobe 651–2180, Japan.*

Received August 24, 2005; accepted October 18, 2005; published online 25, 2005

DNA rich in non-methylated CG motifs (CpGs) enhances induction of immune responses against co-administered antigen encoding genes. CpGs are therefore among the promising adjuvants known to date. However, naked plasmid DNA, even which contains CpG motifs, are taken up by antigen presenting cells *via* the endocytosis pathway. Endocytosed DNAs are thus degraded and their gene expression levels are inefficient. In this context, an effective plasmid delivery carrier is required for DNA vaccine development. We show in the present study that packaging plasmids containing CpGs into fusogenic liposomes (FL) derived from conventional liposomes and Sendai virus-derived active accessory proteins is an attractive method for enhancing the efficacy of a DNA vaccine. These CpG-enhanced plasmids (possessing 16 CpG repeats) that were packaged into FL, enhanced ovalbumin (OVA)-specific T cell proliferation and cytotoxic T cell activity after immunization. In fact, vaccination with CpG enhanced plasmid-loaded FL induced effective prophylactic effects compared with 13 repeats CpG containing plasmid in a tumor challenge experiment. Thus, the development of a CpG-enhanced DNA-FL genetic immunization system represents a promising tool for developing candidate vaccines against some of the more difficult infectious, parasitic, and oncologic disease targets.

Key words DNA vaccine; CpG motif; fusogenic liposome

DNA vaccines have been widely used in laboratory animals and human primates over the last decade to induce humoral and cellular immune responses.[1—5] This approach to immunization has generated sustained interest because of its speed, simplicity, and ability to induce immune responses against naïve protein antigens expressed from plasmid DNA. There has been substantial work on DNA immunization in many species, including humans and large animals.[6—8]

In striking contrast, vaccination with antigen expressing genes usually fails to induce significant immune responses. Various methods are under evaluation to augment the potency of DNA vaccines, such as combination with gene delivery devices to increase the transfection of cells or to target the DNA or with the adjuvants which enhance inflammatory cytokine expression.[9—14] The extent of DNA degradation by extracellular deoxyribonucleases is unknown, but degradation could be considerable. It follows that approaches to protect DNA from the extracellular biological milieu and thereby introduce it into cells more efficiently, should contribute to optimal DNA vaccine design. In this context, not only efficient gene delivery devices but also immunostimulatory adjuvants are essential for augmentation of DNA vaccination.

Interestingly, the sequence composition of plasmid DNA itself also has been shown to increase the potency of the DNA vaccine.[12] This is because the bacterial DNA sequences result in the plasmid which possesses different methylation pattern from mammalian DNA. Bacterial oligonucleotides having the sequence purine–purine–cytosine–guanosine–pyrimidine–pyrimidine, in which the CpG sequence is unmethylated, can activate innate immune system, resulting in an augmentation of the antigen-specific immunity.[15] Recently, it was established that the innate immune system of vertebrates recognizes non methylated CpG motifs flanked by specific bases in bacterial DNA as a danger signal through toll-like receptor 9 (TLR9) expressed on the antigen presenting cells.[16—18] The cytokine profile induced by CpG motifs *in vitro* is consistent with their ability to induce a Th1-biased immune response when used as an adjuvant in vaccine formulations.[19] Therefore, CpG motifs may have potential as adjuvants in protein- and DNA-based vaccine formulations.[20]

CpG DNA is internalized *via* a clathrin dependent endocytic pathway and rapidly moves into a lysosomal compartment.[29] Since it has been known that TLR9 is localized in lysosomal compartment, CpG containing plasmids should be delivered to endosome–lysosome pathway even if plasmids were degraded in endosomes. Recently, several reports are suggested that TLR9 is expressed in ER prior to stimulation and translocate to a CpG containing lysosomal compartment for ligand binding and signal transduction.[29] In this context, with a view of plasmid based DNA vaccine development, CpG DNA targeting to translocating TLR9 is more useful to avoid endosomal DNA degradation.

Previously, we developed a highly unique antigen delivery carrier, fusogenic liposomes (FL), which consist of conventional liposomes and ultra-violet inactivated Sendai virus-derived accessory proteins.[21—24] This carrier could introduce

* To whom correspondence should be addressed. e-mail: nakagawa@phs.osaka-u.ac.jp

its contents into various types of mammalian cells *via* membrane fusion but was not subject to endocytosis. FL introduced encapsulating genes into mammalian cells *in vitro* and *in vivo*. Furthermore, FL mediated DNA immunization induce efficient antigen specific immunity.[25] However, improvement of the efficacy of the FL-mediated gene delivery system is important for the development of a DNA vaccine.

In this study, we, therefore, created a novel genetic immunization system combined with a CpG-containing plasmid backbone and FL. The principal aim of this study was to induce potent antigen-specific immunity to the antigens encoded in the plasmid encapsulated in FL and combined with the CpG motif and a model antigen, chicken egg ovalbumin (OVA), thereby formulating a DNA vaccine.

MATERIALS AND METHODS

Animals and Cells Male C57BL/6 (H-2^b) mice, 7 weeks old, were purchased from SLC Inc. (Hamamatsu, Shizuoka, Japan). EL4 (Tohoku University, Sendai, Japan) is a C57BL/6 T lymphoma and EG7 is an ovalbumin (OVA)-transfected clone of EL4. IC21 cell is a C57BL/6 macrophage clone, H-2Kb. CD8OVA1.3 (provided by Dr. Clifford V. Harding, Case Western Reserve University, Cleveland, OH, U.S.A.) is a T-T hybrid cell, which is specific for OVA257-264-Kb. EL4 and IC21 cells were grown in RPMI1640 medium supplemented with 10% FCS. The CTLL-2 cells were maintained in RPMI1640 medium supplemented with 10% FCS and 1 U/ml human recombinant IL-2. The EG7 cells were maintained in RPMI1640 medium supplemented with 10% FCS and 400 μg/ml G418. CD8OVA1.3 was grown in a DMEM medium supplemented with 10% FCS. All culture media were purchased from Invitrogen (Carlsbad, CA, U.S.A.) and supplemented with non-essential amino acids, antibiotics, and 5×10^5 μM 2-mercaptoethanol (2-ME).

Plasmids The EcoRI fragment of pAc-neo-OVA was cloned into the EcoRI site of pBluescriptII KS(−), resulting in pBluescriptII KS(−)/OVA. To construct an OVA gene expression vector, the BamHI/SalI fragment of pBluescript II KS(−)/OVA was ligated into BamHI/SalI cut pCMV-script (Stratagene), resulting in pCMV-script/OVA (Fig. 1), which is driven by cytomegalovirus promoter and contains a SV40 poly(A) signal. This pCMV-script/OVA containing 13 repeats of the CpG motif, was named pOVACpG13. Furthermore, the plasmid containing 16 CpG motif repeats, pOVACpG16, was constructed as follows. SspI and AlwNI fragments of the pGL3-control vector (Promega) were ligated into pCMV-script digested with AlwNI and blunt ended, resulting in the CpG-enhanced vector, pCMV-script/CpG(+). Then, the BamHI/SalI fragment of pBluescript II KS(−)/OVA was introduced into the BamHI/SalI digested pCMV-script/CpG (+). This plasmid contained 16 CpG motif repeats. Methylated plasmids were prepared by SssI treatment for 4 h at 37 °C. These methylated plasmids were used for experiments after purification by phenol/chloroform precipitation.

Preparation of fusogenic liposome plasmid vector containing unilamellar liposomes was prepared by a modified reverse-phase evaporation method using 46 μmol of lipids (egg phosphatidylcholine : L-α-dimyristryl phosphatidic acid : cholesterol=5 : 1 : 4, molar ratio). After three cycles of freezing and thawing, the liposomes were sized by extrusion through a 0.8 μm polycarbonate membrane (Nucleopore; Coaster, Cambridge, MA, U.S.A.) and pelleted by ultracentrifugation to remove un-encapsulated plasmids. Then, FLs encapsulating pCMV-script/OVA were prepared by fusing the liposomes with UV (2000 J/cm^2)-inactivated Sendai virus as described.[21—24] The amount of plasmid DNA encapsulated within the liposomes was determined by means of fluorometric assay using 3,5-diaminobenzoic acid.

Proliferative Responses of Antigen-Specific T Cells from Immunized Mice Fourteen days after final immunization, lymphocytes were obtained from spleen. B cells were then depleted by using goat anti-mouse IgG (H&L)-coupled micro beads and a MACS column (Miltenyi Biotec, Sunnyvale, CA, U.S.A.). Purified T cells were cultured at a density of 2×10^5 cells/ml with 1 mg/ml OVA for 3 d. To measure cell proliferation, 1 μCi of [^{3}H] thymidine was added to individual culture wells 8 h before termination, and the uptake of [^{3}H] thymidine by dividing cells was determined by scintillation counting.

IL-12 Expression Analysis by ELISA IL-12 levels in culture supernatants of Ag stimulated splenocytes were determined by a cytokine-specific ELISA. Briefly, splenocytes from immunized mice were cultured with 1 mg/ml OVA (or various indicated concentrations). Culture supernatants were harvested 48 h after incubation, and the levels of IL-12 were determined by an IL-12-specific ELISA kit (Biosource). The concentration of cytokines was calculated by standard curves obtained according to the instructions provided by the manufacturer.

***In Vitro* CTL Induction and Cytotoxic Assay** C57BL/6 mice (7 weeks old, male, H-2^b) were immunized twice at 2 week intervals with 50 μg of naked or 5 μg of Fusogenic liposome encapsulated pOVACpG13 or pOVACpG16, respectively. Spleen cells from immunized or non-immunized mice were recovered 14 d after the last immunization and were stimulated *in vitro* with mitomycin C treated EG7 cells for 5 d. The cytotoxic activity of these effector cells was tested on ^{51}Cr-labeled target cells, OVA-expressed EG7 cells, and EL4 as a control, at different effector/target ratios. A cytotoxicity assay was conducted in triplicate. The maximum release was determined by adding 1% Triton X-100 to the target cells. A spontaneous release was obtained in the case of target cells incubated without effector cells. EL4 cells were used as control for specificity. The released radioactivity was measured in the supernatant. The specific lysis was determined as follows:

$$\text{percentage of specific lysis} = 100\times[(\text{release of CTLs})-(\text{spontaneous release})]/[(\text{maximal release})-(\text{spontaneous release})]$$

Tumor Challenge Experiments C57BL/6 mice (7 weeks old, male, H-2b) were immunized s.c. at the tail base twice at 2 week intervals with 50 μg of naked or 5 μg of fusogenic liposome encapsulated pOVACpG13 or pOVACpG16. Fourteen days after the last immunization (day 0), 1×10^6 OVA expressing EG7 cells were intradermally injected. Six to 13 mice were used for each experimental group. Tumor survival in tumor bearing mice was monitored weekly. Mice that developed tumors larger than 4000 mm^3 were considered to have developed lethal tumors.

RESULTS

***In Vitro* Enhancement of IL-12 Expression by CpG-Enhanced Vectors Combined with FL** Initially we evaluated the immunostimulatory effect of CpG-enhanced vector encapsulated in FL by IL-12 production (Fig. 1). ELISA analysis showed that IL-expression of FL/pOVACpG16-stimulated splenocytes tended to enhance IL-12 production compared with non-CpG enhanced vector (pOVACpG13) containing FL. In addition, methylated plasmid vector encapsulated in FL or empty FL did not enhance IL-12 expression. These results clearly showed that CpG-enhanced vectors retained their immunostimulatory effect even when encapsulated in FL, and IL-12 expression increased depending on the number of CpG motifs.

Vaccination with CpG-Enhanced Vector Combined with FL Significantly Enhances Antigen Specific T Cell Mediated Immune Responses in Vaccinated Mice Examination of antigen-specific proliferation of lymphocytes in immunized mice (Fig. 2) indicated that FL/pOVACpG16 vaccination dramatically enhanced proliferation. On the other hand, FL/pOVACpG13- or naked CpG-enhanced or non-enhanced vector immunization did not induce antigen-specific proliferation. These results indicated that the combination of CpG immuno stimulatory sequences and FL significantly enhanced antigen specific T cell proliferation under a very low dose (5 μg). Next, the immunogenicity of FL/pOVACpG16 was tested by CTL assay (Fig. 3). The best response was obtained for pOVACpG16 combined with FL, which exhibited *ex vivo* killing of *ca.* 40% at an E : T ratio of 50. The corresponding killing obtained by pOVACpG13 combined with FL was in the range of 30%.

Protection against the Growth of OVA-Expressing Tumors in Mice Vaccinated with CpG-Enhanced Vectors by FL To determine whether the observed enhancement in antigen-specific T cell mediated immunity translated to a significant anti-tumor immunity and prolonged survival, we performed an *in vivo* tumor protection experiment using an OVA expressing tumor-model, EG7. As shown in Fig. 4, 70% of mice receiving the pOVACpG16 vaccine combined with FL survived 90 d after the EG7 challenge. In contrast, the survival rate of unvaccinated mice and mice receiving pOVACpG13 or pOVACpG16 alone or a combination vaccine of pOVACpG13 and FL was less than 40%. A two-fold improvement was observed in the response of mice treated with a prophylactic vaccine treatment consisting of pOVACpG16 combined with FL. These results indicated that the combination of CpG enhanced vectors and FL was a more effective genetic immunization system for prophylactic tumor vaccine.

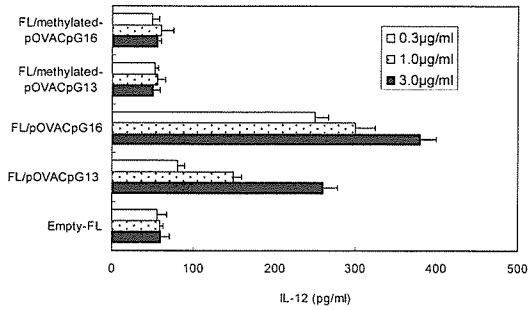

Fig. 1. CpG Enhanced Vector (pOVACpG16) Containing FL Hold Immunostimulatory Effects

Splenocytes from naïve mice were cultured for 2 d in the presence of FL-pOVACpG13, FL-pOVACpG16, FL-methylated pOVACpG13 and FL-methylated pOVACpG16 at indicated concentrations. Then IL-12 levels in the culture supernatants were determined by ELISA.

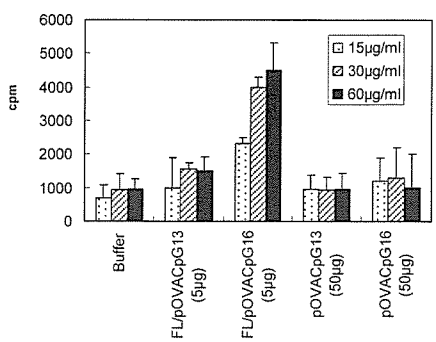

Fig. 2. OVA Specific T Cell Proliferation Derived from Mice Splenocytes Immunized with CpG Enhanced FL-DNA Vaccine

Spleen cells from C57/Bl6 mice immunized with balanced salt solution (Buffer), 5 μg FL-pOVACpG13, 5 μg FL-pOVACpG16, 50 μg pOVACpG13 and 50 μg pOVACpG16 were assayed for proliferation assay. Then the splenocytes were incubated with 15 (□), 30(▨), 60(■) μg/ml OVA in culture medium for 3 d. OVA specific proliferative responses were determined by [^{3}H]-thymidine uptake.

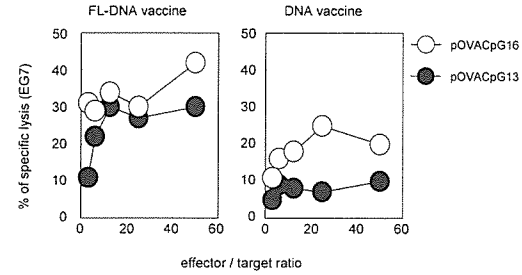

Fig. 3. OVA Specific CTL Response after *in Vivo* Priming with CpG Enhanced FL-DNA Vaccine

Spleen cells from C57/Bl6 mice that had been immunized with 50 μg FL-pOVACpG13, 50 μg FL-pOVACpG16, 5 μg pOVACpG13, 5 μg pOVACpG16 were assayed for cytotoxic activity, after *in vitro* stimulation with EG7 tumor cells for 5 d. The figure represents the amount of specific lysis against the 51Cr labeled EG7 cells.

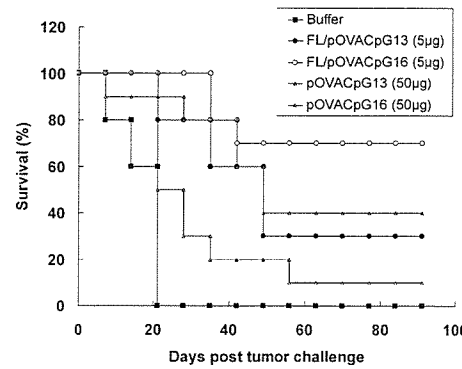

Fig. 4. Survival Analysis of Mice Immunized with DNA-Fusogenic Liposome Vaccine in a Prophylactic Treatment Model

C57/Bl6 mice were immunized with Buffer, 50 μg pOVACpG13 or 50 μg pOVACpG16 as control vaccine, 5 μg FL-pOVACpG13 or 5 μg FL-pOVACpG16 twice with an interval of two weeks between treatments. Four weeks after last immunization, immunized mice were challenged i.d. in the abdomen with 1×10^6 cells. Comparison of survival curves of two groups were significantly different ($p<0.01$).

DISCUSSION

In the present study, we demonstrated that a combination of CpG-enhanced vectors and FL strengthened IL-12 expression by splenocytes from naïve mice, and this approach enhanced the potency of DNA vaccines using OVA as a model antigen, leading to effective OVA specific T cell proliferation, CTL responses, and prophylactic anti-tumor effects. Our previous study showed that immunization of mice with conventional OVA expression vector, pOVACpG13 using FL, induced antigen-specific antibodies and strong CTL responses.[25] In the present study, we utilized CpG immunostimulatory sequences to enhance FL-mediated DNA vaccination therapy. The results demonstrated that CpG introduction was effective for *in vitro* inflammatory cytokine production by APCs and this leads to dramatically enhanced proliferation of antigen-specific T cell proliferation, because IL-12 production and OVA specific T cell proliferation was significantly weaker in conventional CpG containing plasmid vector (pOVACpG13) or even in combination with FL in immunized mice.

Generally, the CpG motif, even in a plasmid backbone, stimulates APCs *via* TLR9 receptor signaling.[16,17] Although these activation mechanisms are available to the endocytosis pathway,[26] previous studies have not reported any investigations of immunostimulatory ability of directly introduced CpG motifs *via* membrane fusion. Recent report suggested that TLR is expressed in ER prior to stimulation, and translocate to lysosomal compartment through cytosolic compartment by inflammatory stimuli.[29] So we hypothesized that CpG enhanced plasmid in cytosol could bind to TLR9, which is translocating from ER to lysosome through cytosol. Another hypothesis is that DNAs adsorbed on FL or released from FL may interact with TLR9. Overall, although our data indicate that the direct introduction of CpG-enhanced vectors *via* membrane fusion retained their stimulatory effects, detailed studies are needed to clarify activation mechanisms. Our data indicated that antigen specific T cell proliferation and CTL responses were more effective than the combination of FL and conventional pOVACpG13 in vaccinated mice. When challenged with OVA-expressing EG7 tumors, mice immunized with the CpG-enhanced vector combined with FL exhibited prolonged survival compared with conventional vector immunized groups, even when combined with FL.

Although the anti-tumor effects presented in Fig. 4 are somewhat striking, they hold little relevance to immunological therapy against tumors. We should have tested their vaccines in a therapeutic mode (tumor first and vaccine after) and not solely in a prophylactic fashion. Moreover, these experiments do not address the issue of potential immunological tolerance to real tumor antigens, which in many cases are also expressed to some extent by normal cells, since OVA is a totally foreign antigen. Studies conducted using a real tumor antigen in murine models, such as TRP2 for B16 melanoma,[27] P1A for P815 mastocytoma,[28] or anything equivalent, could potentially provide additional information that better simulates actual conditions.

In summary, our findings indicate that the introduction of three CpG immunostimulatory sequences and FL is able to enhance inflammatory cytokines and elicit more effective antigen-specific T cell activity and prophylactic anti-tumor effects *in vivo* than a previously developed conventional plasmid backbone (pOVACpG13 and FL combination vaccine). This approach may be promising for future vaccine development to control cancer, which expresses self antigens, or infectious diseases, and may be particularly useful in patients with reduced immune responses, particularly human immunodeficiency virus (HIV) or human T cell leukemia virus (HTLV)-infected patients. Studies are in progress to clarify the efficacy of FL mediated genetic immunization systems on tumor-associated antigens and virus-related antigen expression vectors.

Acknowledgements We are grateful to Mr. M. Mori and Mr. K. Sakaguchi at NOF Corporation for supplying us with lipid mixture. This study was supported in part by Core Research for the Evolutional Science and Technology Program, Japan Science and Technology Corp., and the Ministry of Education, Culture, Sports, Science, and Technology, Japan.

REFERENCES

1) Ulmer J. B., Donnelly J. J., Parker S. E., Rhodes G. H., Felgner P. L., Dwarki V. J., Gromkowski S. H., Deck R. R., DeWitt C. M., Friedman A., *et al.*, *Science*, **259**, 1745—1749 (1993).
2) Corr M., von Damm A., Lee D. J., Tighe H., *J. Immunol.*, **163**, 4721—4727 (1999).
3) Donnelly J. J., Ulmer J. B., Shiver J. W., Liu M. A., *Annu. Rev. Immunol.*, **15**, 617—648 (1997).
4) Donnelly J. J., Ulmer J. B., Liu M. A., *Dev. Biol. Stand.*, **95**, 43—53 (1998).
5) Montgomery D. L., Ulmer J. B., Donnelly J. J., Liu M. A., *Pharmacol. Ther.*, **74**, 195—205 (1997).
6) Donnelly J. J., Friedman A., Martinez D., Montgomery D. L., Shiver J. W., Motzel S. L., Ulmer J. B., Liu M. A., *Nat. Med.*, **1**, 583—587 (1995).
7) MacGregor R. R., Boyer J. D., Ugen K. E., Lacy K. E., Gluckman S. J., Bagarazzi M. L., Chattergoon M. A., Baine Y., Higgins T. J., Ciccarelli R. B., Coney L. R., Ginsberg R. S., Weiner D. B., *J. Infect. Dis.*, **178**, 92—100 (1998).
8) Wang R., Epstein J., Baraceros F. M., Gorak E. J., Charoenvit Y., Carucci D. J., Hedstrom R. C., Rahardjo N., Gay T., Hobart P., Stout R., Jones T. R., Richie T. L., Parker S. E., Doolan D. L., Norman J., Hoffman S. L., *Proc. Natl. Acad. Sci. U.S.A.*, **98**, 10817—10822 (2001).
9) Singh M., Kazzaz J., Ugozzoli M., Chesko J., O'Hagan D. T., *Expert. Opin. Biol. Ther.*, **4**, 483—491 (2004).
10) O'Hagan D., Singh J., Ugozzoli M., Wild C., Barnett S., Chen M., Schaefer M., Doe B., Otten G. R., Ulmer J. B., *J. Virol.*, **75**, 9037—9043 (2001).
11) Roy K., Mao H. Q., Huang S. K., Leong K. W., *Nat. Med.*, **5**, 387—391 (1999).
12) Ulmer J. B., DeWitt C. M., Chastain M., Friedman A., Donnelly J. J., McClements W. L., Caulfield M. J., Bohannon K. E., Volkin D. B., Evans R. K., *Vaccine*, **18**, 18—28 (1999).
13) Nakanishi T., Kunisawa J., Hayashi A., Tsutsumi Y., Kubo K., Nakagawa S., Nakanishi M., Tanaka K., Mayumi T., *J. Control. Release*, **61**, 233—240 (1999).
14) Nakanishi T., Kunisawa J., Hayashi A., Tsutsumi Y., Kubo K., Nakagawa S., Fujiwara H., Hamaoka T., Mayumi T., *Biochem. Biophys. Res. Commun.*, **240**, 793—797 (1997).
15) Krieg A. M., Yi A. K., Matson S., Waldschmidt T. J., Bishop G. A., Teasdale R., Koretzky G. A., Klinman D. M., *Nature* (London), **374**, 546—549 (1995).
16) Hemmi H., Kaisho T., Takeda K., Akira S., *J. Immunol.*, **170**, 3059—3064 (2003).
17) Hemmi H., Takeuchi O., Kawai T., Kaisho T., Sato S., Sanjo H., Matsumoto M., Hoshino K., Wagner H., Takeda K., Akira S., *Nature* (London), **408**, 740—745 (2000).
18) Akira S., Hemmi H., *Immunol. Lett.*, **85**, 85—95 (2003).

19) Brazolot Millan C. L., Weeratna R., Krieg A. M., Siegrist C. A., Davis H. L., *Proc. Natl. Acad. Sci. U.S.A.*, **95**, 15553—15558 (1998).
20) Krieg A. M., *Biochim. Biophys. Acta*, **1489**, 107—116 (1999).
21) Kunisawa J., Nakanishi T., Takahashi I., Okudaira A., Tsutsumi Y., Katayama K., Nakagawa S., Kiyono H., Mayumi T., *J. Immunol.*, **167**, 1406—1412 (2001).
22) Mizuguchi H., Nakagawa T., Nakanishi M., Imazu S., Nakagawa S., Mayumi T., *Biochem. Biophys. Res. Commun.*, **218**, 402—407 (1996).
23) Nakanishi T., Hayashi A., Kunisawa J., Tsutsumi Y., Tanaka K., Yashiro-Ohtani Y., Nakanishi M., Fujiwara H., Hamaoka T., Mayumi T., *Eur. J. Immunol.*, **30**, 1740—1747 (2000).
24) Sugita T., Yoshikawa T., Gao J. Q., Shimokawa M., Oda A., Niwa T., Akashi M., Tsutsumi Y., Mayumi T., Nakagawa S., *Biol. Pharm. Bull.*, **28**, 192—193 (2005).
25) Yoshikawa T., Imazu S., Gao J. Q., Hayashi K., Tsuda Y., Shimokawa M., Sugita T., Niwa T., Oda A., Akashi M., Tsutsumi Y., Mayumi T., Nakagawa S., *Biochem. Biophys. Res. Commun.*, **325**, 500—505 (2004).
26) Ahmad-Nejad P., Hacker H., Rutz M., Bauer S., Vabulas R. M., Wagner H., *Eur. J. Immunol.*, **32**, 1958—1968 (2002).
27) Brichard V., Van Pel A., Wolfel T., Wolfel C., De Plaen E., Lethe B., Coulie P., Boon T., *J. Exp. Med.*, **178**, 489—495 (1993).
28) Lethe B., van den Eynde B., van Pel A., Corradin G., Boon T., *Eur. J. Immunol.*, **22**, 2283—2288 (1992).
29) Latz E., *et al.*, *Nat. Immunol.*, **5**, 190—198 (2004).

Available online at www.sciencedirect.com
ScienceDirect
PLACENTA
ELSEVIER
Placenta 27 (2006) 934–938

Technical Note

Characteristics of Transcription-regulatory Elements for Gene Expression from Plasmid Vectors in Human Trophoblast Cell Lines

E. Komiya [a], M. Kondoh [a,c,*], H. Mizuguchi [b,c], M. Fujii [a], N. Utoguchi [d], T. Nakanishi [e], Y. Watanabe [a]

[a] *Department of Pharmaceutics and Biopharmaceutics, Showa Pharmaceutical University, Machida, Tokyo 194-8543, Japan*
[b] *Laboratory of Gene transfer and Regulation, National Institute of Biomedical Innovation, Osaka 565-0085, Japan*
[c] *Graduate School of Pharmaceutical Sciences, Osaka University, Suita 565-0871, Japan*
[d] *Department of Biopharmaceutics, School of Pharmaceutical Sciences, Teikyo University, Kanagawa 199-0195, Japan*
[e] *Department of Toxicology, Graduate School of Pharmaceutical Sciences, Osaka University, Suita 565-0871, Japan*

Accepted 7 February 2006

Abstract

Nonviral gene delivery systems are useful for basic research in trophoblasts. In these systems, gene expression is regulated by a cassette of regulatory elements within the plasmid, and the transcriptional activity differs among cell lines. In the present study, we used BeWo and JAR human trophoblast cell lines to systematically compare the transcriptional activities of several expression cassettes and those of a control plasmid made up of a simian virus 40 (SV40) promoter, a polyadenylation (PA) signal, and an enhancer. We also found that insertion of intron elements enhanced transcriptional activities in the following order: intron A > hybrid β-globin-immunoglobin intron > no intron. Of several PA signals tested including those from SV40, bovine growth hormone, and the minimal rabbit β-globin, the latter had the highest transcriptional activities (3.9- and 26-fold over control plasmid in BeWo and JAR cells, respectively). Addition of a second enhancer increased the transcriptional activity in these cells. We also found that gene expression level can be controlled by selecting the expression cassette. These results should be useful for further transgene experiments in BeWo and JAR cells.

Keywords: Trophoblast cell lines; Gene expression; Plasmid vector; Nonviral vector

1. Introduction

Techniques for transducing genes are useful for basic research of placenta. Gene transduction can be accomplished using either nonviral or viral vectors. Cationic lipid and adenovirus vector are representative nonviral and viral vectors, respectively. The adenovirus vector has a much higher efficiency of transfection than cationic lipids; 100- to 1000-fold more DNA is needed to obtain the same level of transgene activity using cationic lipids compared to the adenovirus vector [1]. Two disadvantages of the adenovirus vector, however, are that the size of transgene is limited [2], and that preparation of the vector is complicated. Moreover, side-effects caused by viral components, including proteins and nucleic acids, are inevitable. In contrast, with nonviral vectors, the size of the transgene is not limited, there is less toxicity, and, moreover, they are easy to prepare.

In addition to overcoming the low efficiency of transgene transfection with cationic lipids, there is also a problem of dose-dependent toxicity of cationic lipid–DNA complexes. Two approaches for solving these problems include the development of lipids with less toxicity, several of which have been

Abbreviations: SV40, Simian virus; PA, Polyadenylation signal; BGH, Bovine growth hormone; mRBG, Minimal rabbit β-globin; Chimeric, Hybrid intron of β-globin and immunoglobin; CMV, Human cytomegalovirus immediate early 1 gene; Intron A, The largest intron human CMV immediate early 1 gene; PGK, Phosphoglycerate kinase.

* Corresponding author. Department of Pharmaceutics and Biopharmaceutics, Showa Pharmaceutical University, Machida, Tokyo 194-8543, Japan. Tel.: +81 42 721 1556; fax: +81 42 723 3585.
E-mail address: masuo@ac.shoyaku.ac.jp (M. Kondoh).

0143-4004/$ - see front matter © 2006 Elsevier Ltd. All rights reserved.
doi:10.1016/j.placenta.2006.02.007

reported [1,3,4], and improvement of transcriptional activity. Transcription in mammalian cells is regulated by regulatory DNA sequences, including promoters, introns, polyadenylation (PA) signals, and enhancers. Optimal transgene expression depends on the expression cassette and components in a plasmid, and several reports have shown that the optimal cassette depends on the cell line [5–9]. Therefore, it is important to systematically evaluate the various sequence elements that contribute to high-level expression.

Human trophoblast cell lines BeWo and JAR are widely used for basic studies of human placenta [10–12]. Because transgenic experiments are promising for studies of placenta, it is necessary to optimize expression cassettes for BeWo and JAR cells; however, the various regulatory elements have not been systematically analyzed. Therefore, in the present study, we systematically investigated the effects of several expression cassettes on transgene activity in BeWo and JAR cells.

2. Materials and methods

2.1. Cell cultures

Human choriocarcinoma cell lines BeWo and JAR cells were used in this study. BeWo cells were maintained in Dulbecco's modified Eagle's medium with 10% fetal bovine serum, 2 mM L-glutamine, 1.44 g/l $NaHCO_3$, and 3.15 g/l D-glucose and 0.1 mM MEM nonessential amino acid solution. JAR cells were cultured in RPMI 1640 medium containing 10% fetal bovine serum, 1 mM pyruvate, 2.14 g/l HEPES, 1.35 g/l $NaHCO_3$, and 4.05 g/l D-glucose. All cells were incubated in a 5% CO_2 atmosphere at 37 °C.

2.2. Plasmids

To optimize gene cassette expression, we previously prepared several derivatives of the firefly luciferase-expressing plasmid pGL-3 (Promega, Madison, WI) containing the promoter, PA signal, and enhancer sequences from SV40 [7]. In this study, we also used the plasmids listed in Table 1. Plasmids were purified using a Maxi or Midi kit (Qiagen, Valencia, CA) according to the manufacturer's instructions.

2.3. Transfection assay

The cells were seeded on 24-well plates at 8×10^4 cells per well. On the following day, each plasmid (0.2 μg/well) was transfected using Effectene reagent (Qiagen) according to the manufacturer's instructions. After 24 h of transfection, the cells were recovered, and luciferase activity in the cells was determined using a commercially available assay kit (PicaGene LT2.0; Toyo Inki Co., Tokyo, Japan). The protein content in the cells was determined with a bicinchoninic acid assay kit using bovine serum albumin as a standard (Pierce Chemical Co., Rockford, IL). The luciferase activities were calculated from the relative luminescent units per μg protein. The activities were normalized by the luciferase activity in cells transfected with unmodified pGL-3 vector. At least two independent plasmid preparations were used for each experiment.

Table 1
Structures of plasmids used in this study

Plasmids	Promoter	Intron	PA	Enhancer
pGL-3	SV40	–	SV40	SV40
pCMVL1	CMV	–	BGH	CMV
pPGKL	PGK	–	BGH	–
pCMVL2-1	CMV	Chimeric	BGH	CMV
pCMVL3-1	CMV	Intron A	BGH	CMV
pCAL3	β-actin	β-actin	SV40	CMV
pCAL3-1	β-actin	β-actin	BGH	CMV
pCAL3-2	β-actin	β-actin	mRBG	CMV
pCASL3	β-actin	β-actin	SV40	CMV + SV40

2.4. Statistical analysis

Statistical analysis was performed using one-way ANOVA, followed by Dunnett's method. The level of significance was set at $p < 0.05$.

3. Results

3.1. Effect of promoter sequences on transgene expression in BeWo and JAR cells

To compare promoter strength, we tested several plasmids containing different promoters (simian virus (SV40), human cytomegalovirus immediate early 1 gene (CMV), and phosphoglycerate kinase (PGK)). As shown in Fig. 1, the transcriptional activities were the same for all three promoters in BeWo cells (Fig. 1A), but the transcriptional activity for the PGK promoter was 11.7-fold higher than the SV40 and CMV

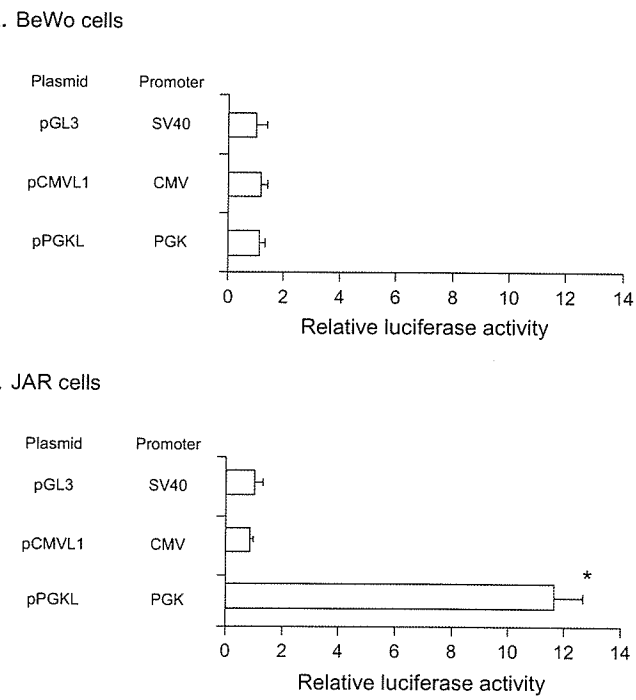

Fig. 1. Effect of promoter sequences on transgene expression in BeWo and JAR cells. BeWo cells (A) or JAR cells (B) were seeded on 24-well plates at 8×10^4 cells per well. Cells were transfected with the plasmid vector containing SV40, CMV or PGK promoter (Table 1) (0.2 μg/well) using Effectene transfection reagent, and after 24 h of culture, the cells were harvested and lysed with a commercially available lysis buffer (LCβ). The luciferase activity was measured, and the activity was normalized by the protein content. The luciferase levels are expressed in comparison to the control plasmid vector pGL-3. The results represent means ± SD ($n = 4$) and are representative of at least three independent experiments using at least two independent plasmid preparations. *Significantly different from the pGL-3 control plasmid ($p < 0.05$).

promoters in the JAR cells (Fig. 1B), indicating that the transcriptional factors may differ between BeWo and JAR cells.

3.2. Effect of intron sequences on transgene expression in BeWo and JAR cells

Previous reports have shown that the inclusion of heterologous introns in expression plasmids increases their expression in cultured cells [7,9,13]. We investigated the effects of intron A and a chimeric intron composed of the 5′-donor splice site from the human β-globin intron 1 and the 3′-acceptor splice site from the intron of an immunoglobin gene heavy chain variable region. The intron sequences were inserted into a luciferase-expressing plasmid containing the CMV promoter, the bovine growth hormone (BGH) PA signal, and the CMV enhancer. The plasmid was transduced into the cells using Effectene transfection reagent, and after 24 h of culture, the luciferase activity was measured. As shown in Fig. 2A, in BeWo cells, insertion of the introns resulted in elevation of gene expression (3.7-fold for the insertion of the chimeric intron and 6.6-fold for the insertion of intron A). Similar results were obtained in JAR cells (5.2-fold in chimeric introns and 18.4-fold in intron A; Fig. 2B).

3.3. Effect of PA signals on transgene expression in BeWo and JAR cells

To determine whether insertion of the PA sequence affects gene expression, we compared three different PA signals derived from the rabbit β-globin gene, the SV40 late genome, and the BGH gene. The SV40 and BGH PA signals are commonly used in expression vectors, and the β-globin PA signal has been shown to be efficiently recognized in mammalian cells [14]. The minimal rabbit β-globin PA signal was reported to be more efficiently recognized than the SV40 PA signal [15]. As shown in Fig. 3A and B, insertion of most of the PA signals elevated gene expression in BeWo and JAR cells, although their activities differed. The most efficient PA signal was that from mRBG (3.9-fold in BeWo cells and 26-fold in JAR cells). Although the SV40 and BGH signals were relatively ineffective in BeWo cells, they increased luciferase expression by approximately 8-fold over the control values.

3.4. Effect of a second enhancer on transgene expression in BeWo and JAR cells

Enhancers are binding sites for eukaryotic gene activators located upstream or downstream from promoter sequences.

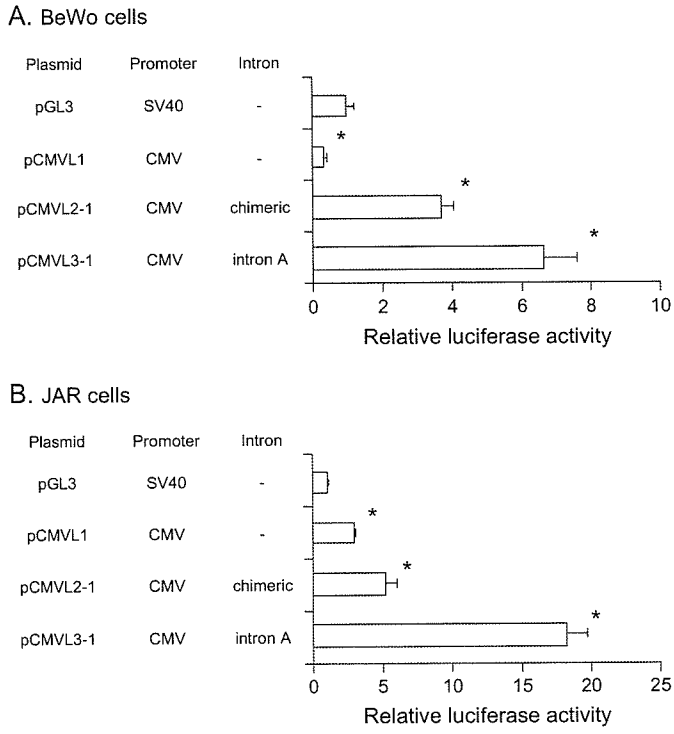

Fig. 2. Effect of intron sequences on transgene expression in BeWo and JAR cells. BeWo cells (A) or JAR cells (B) were transfected with the plasmid vector containing intron A or chimeric intron (Table 1) as described in the legend of Fig. 1. After 24 h of culture, the cells were harvested and lysed with a commercially available lysis buffer (LCβ). The luciferase activity was then measured as described in the legend of Fig. 1. The results represent means ± SD ($n = 4$) and are representative of at least three independent experiments using at least two independent plasmid preparations. *Significantly different from the pGL-3 control plasmid ($p < 0.05$).

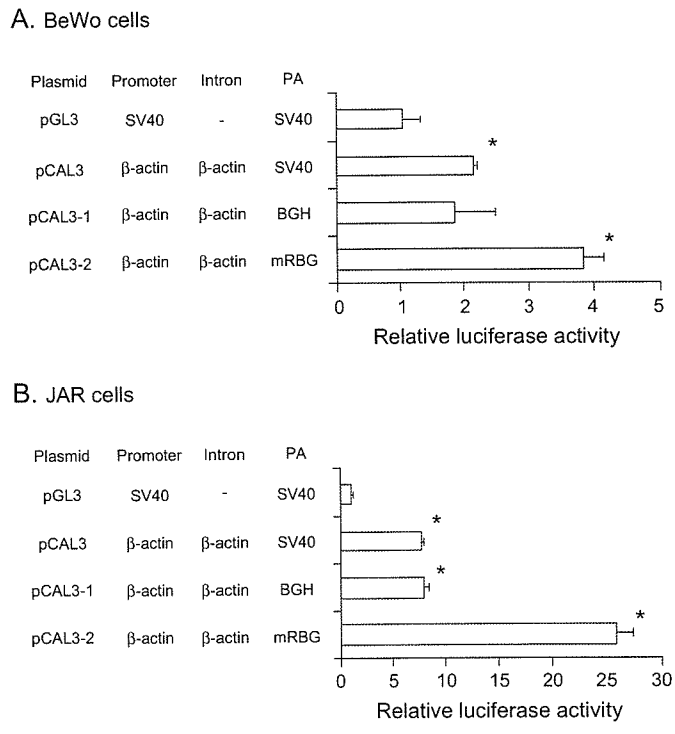

Fig. 3. Effect of PAs on transgene activity in BeWo and JAR cells. BeWo cells (A) or JAR cells (B) were transfected with the plasmid vector containing SV40, BGH or mRBG PA signal (Table 1) as described in the legend of Fig. 1. After 24 h of culture, the cells were harvested and lysed with a commercially available lysis buffer (LCβ). The luciferase activity was measured as described in the legend of Fig. 1. The results represent means ± SD ($n = 4$) and are representative of at least three independent experiments using at least two independent plasmid preparations. *Significantly different from the pGL-3 control plasmid ($p < 0.05$).